Introduction to Quantitative XRF analysis

Andreas - Germanos Karydas

***NSIL-**Nuclear Science and Instrumentation Laboratory*
*International Atomic Energy Agency (**IAEA**)*
***IAEA Laboratories**, A-2444 Seibersdorf, Austria*
A.Karydas@iaea.org

Outline

- Basic mechanisms for ionization/fluorescence process
- Primary XRF Intensity
- Indirect enhancement processes of XRF intensity
- XRF analysis in the real world:
  - Non-parallel exciting beams
  - Influence of surface topography
  - Geometrical considerations
  - Particle size effects

Interaction of X-rays with atoms

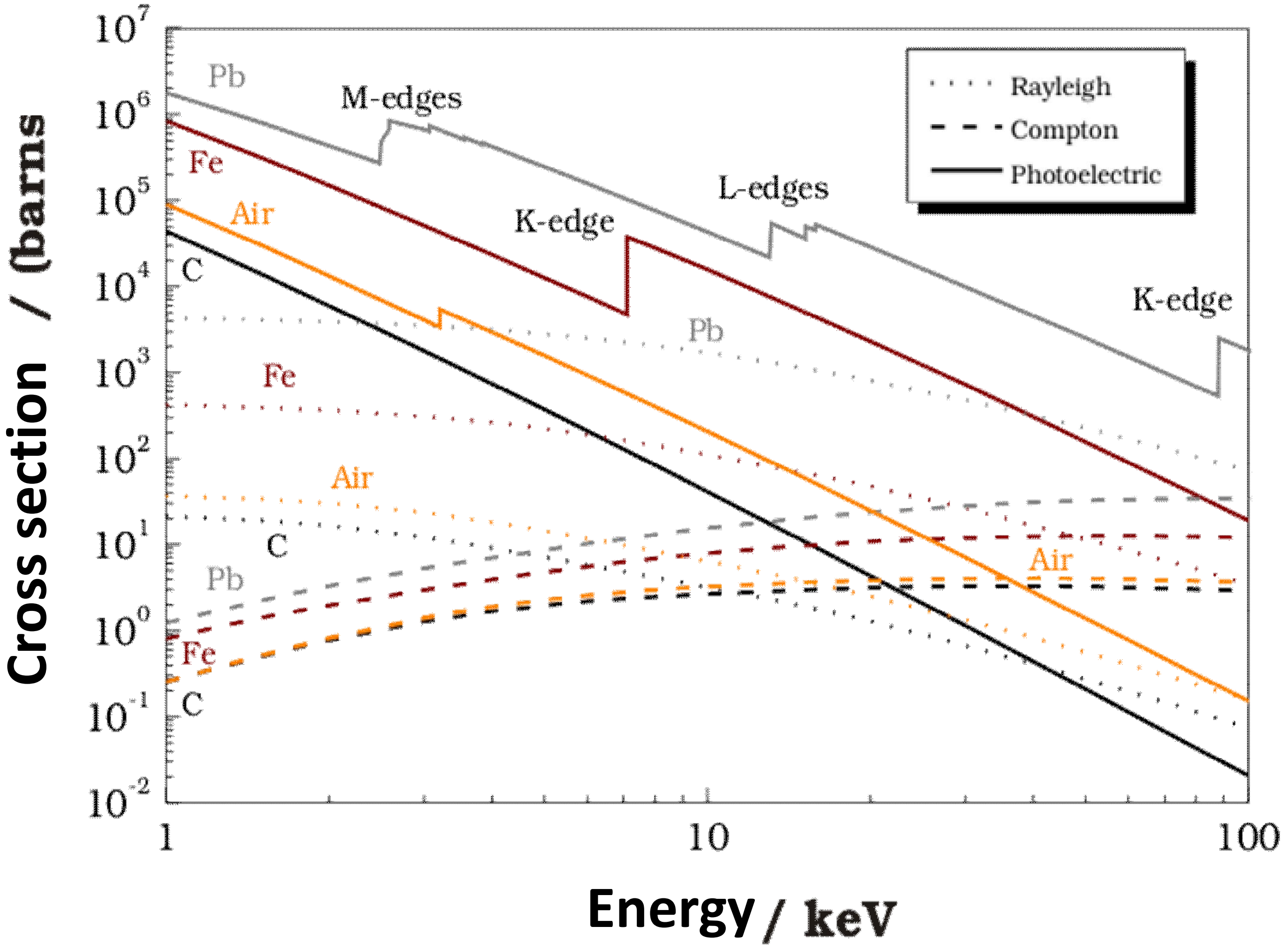

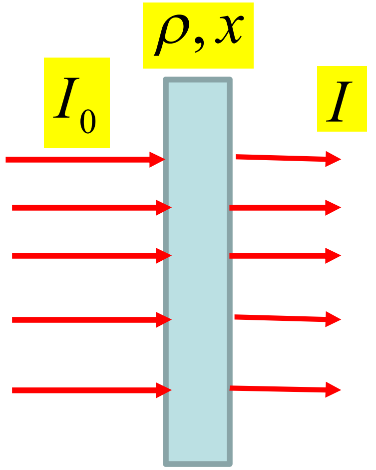

$$I = I_0 \cdot e^{-(\tau+\sigma_R+\sigma_C)\cdot\rho\cdot x}$$

Photoelectric cross sections

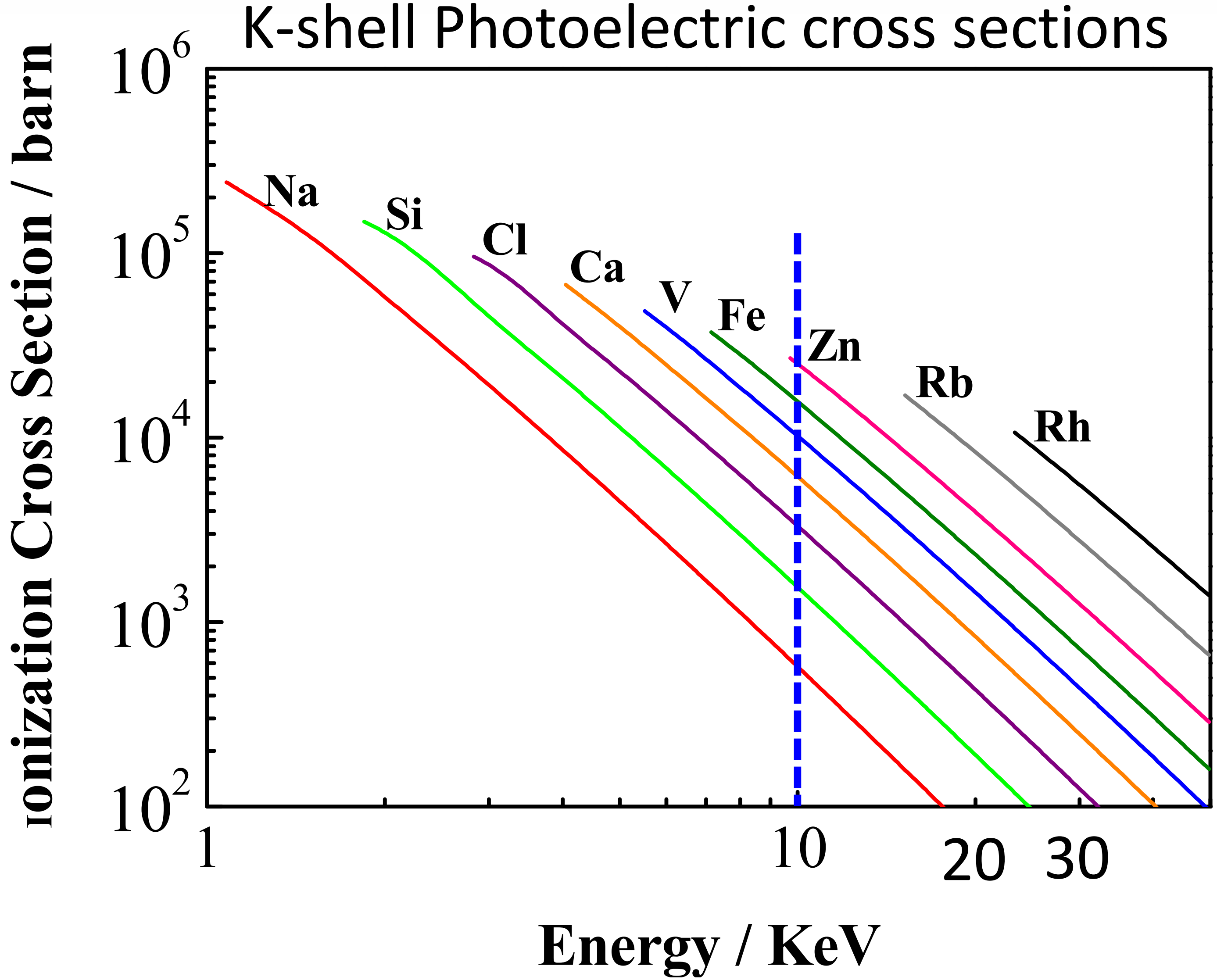

10^4-10^5 b

Photon ICS from "Elam database" Elam W.T. et al., *Radiat. Phys. Chem, 63,* (2002), 121

Photoelectric cross section:

$$\tau \sim E^{-3.5}$$

$$\tau \sim Z^{3\ to\ 4}$$

X-ray Scattering Interactions with atoms

E_0>>Binding Energy

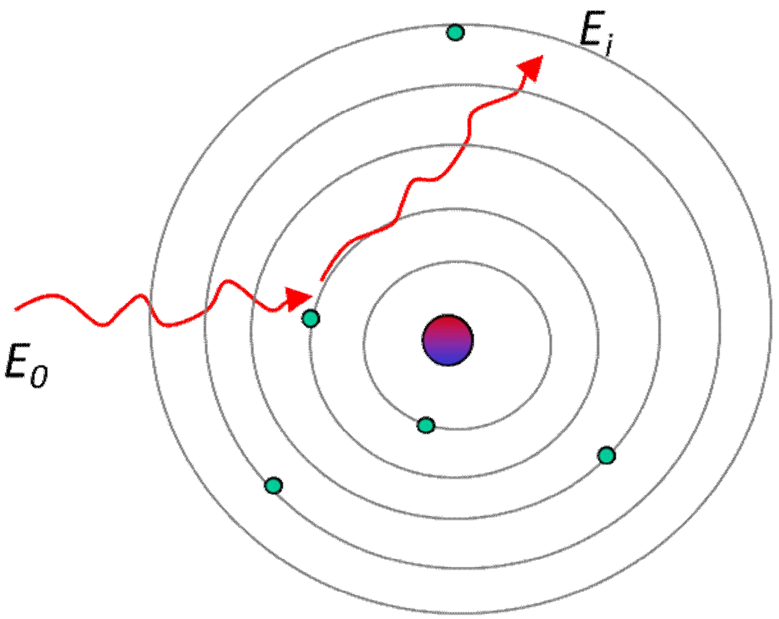

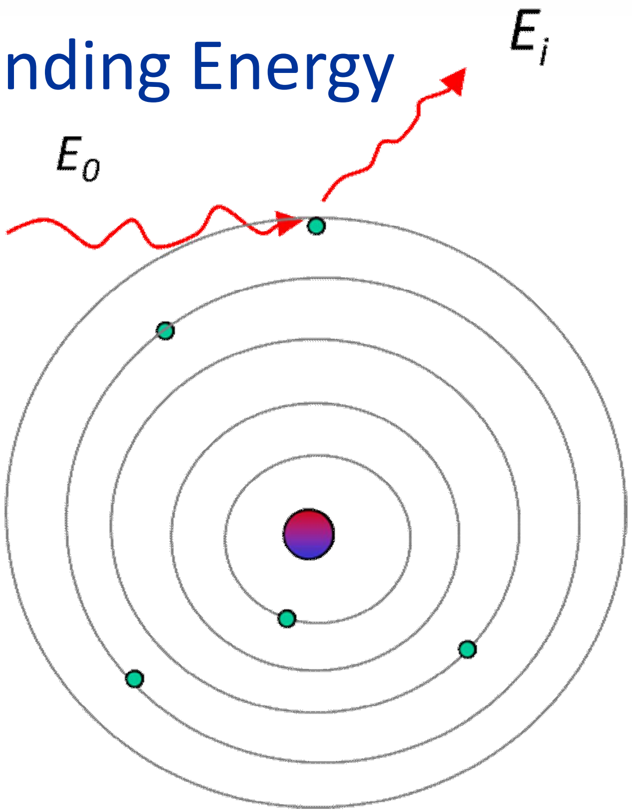

***E_i=E_0* : Coherent (Rayleigh),** mostly with inner atomic electrons

E_i < E_0: Incoherent (Compton), mostly with outer, less bound electrons

Scattering probabilities: Unpolarized excitation

Z	WF (%)
Al	8.4
Si	26.7
Ca	9.3
Fe	9.8

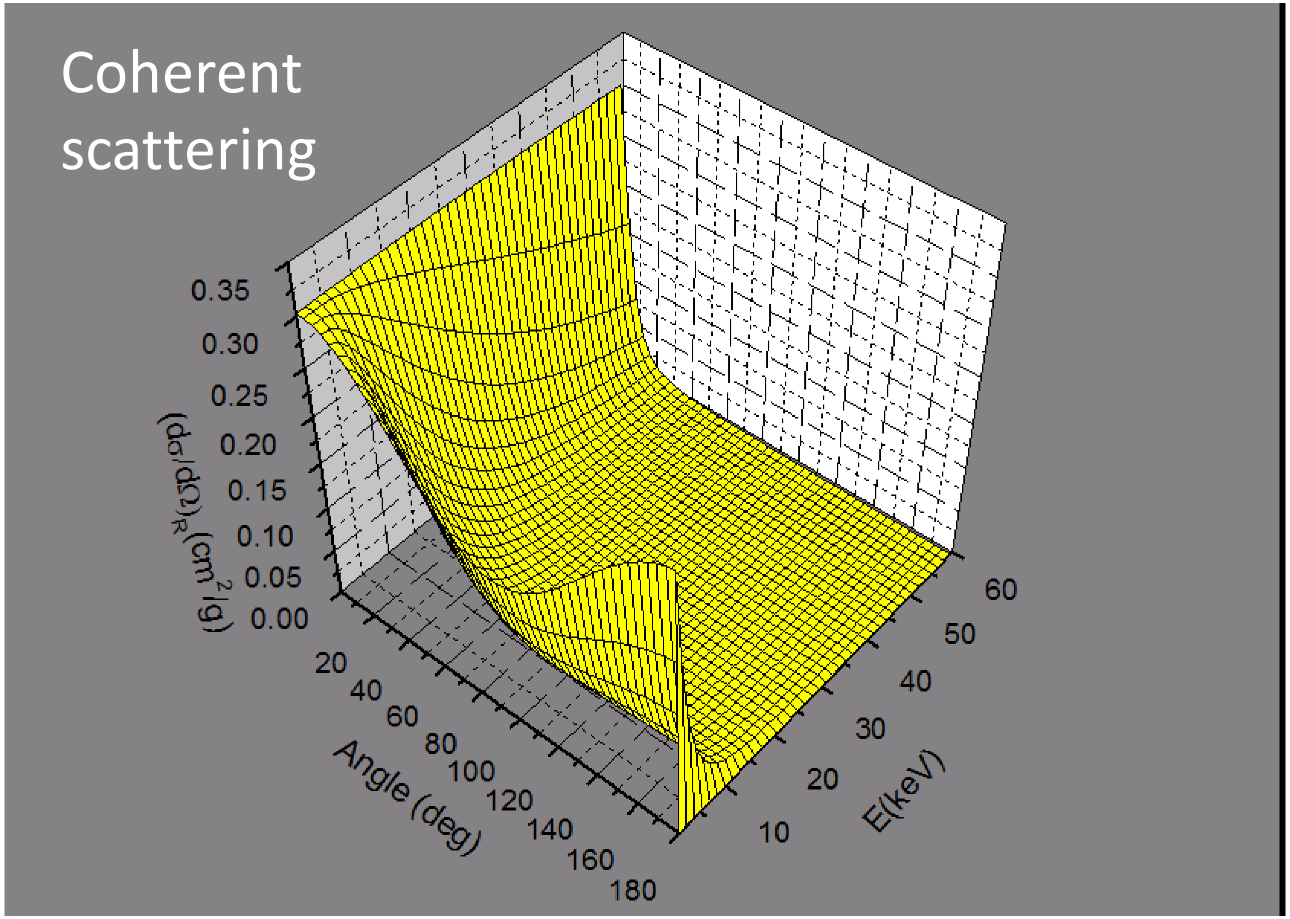

Scattering probabilities: Unpolarized excitation

Z	WF (%)
Al	8.4
Si	26.7
Ca	9.3
Fe	9.8

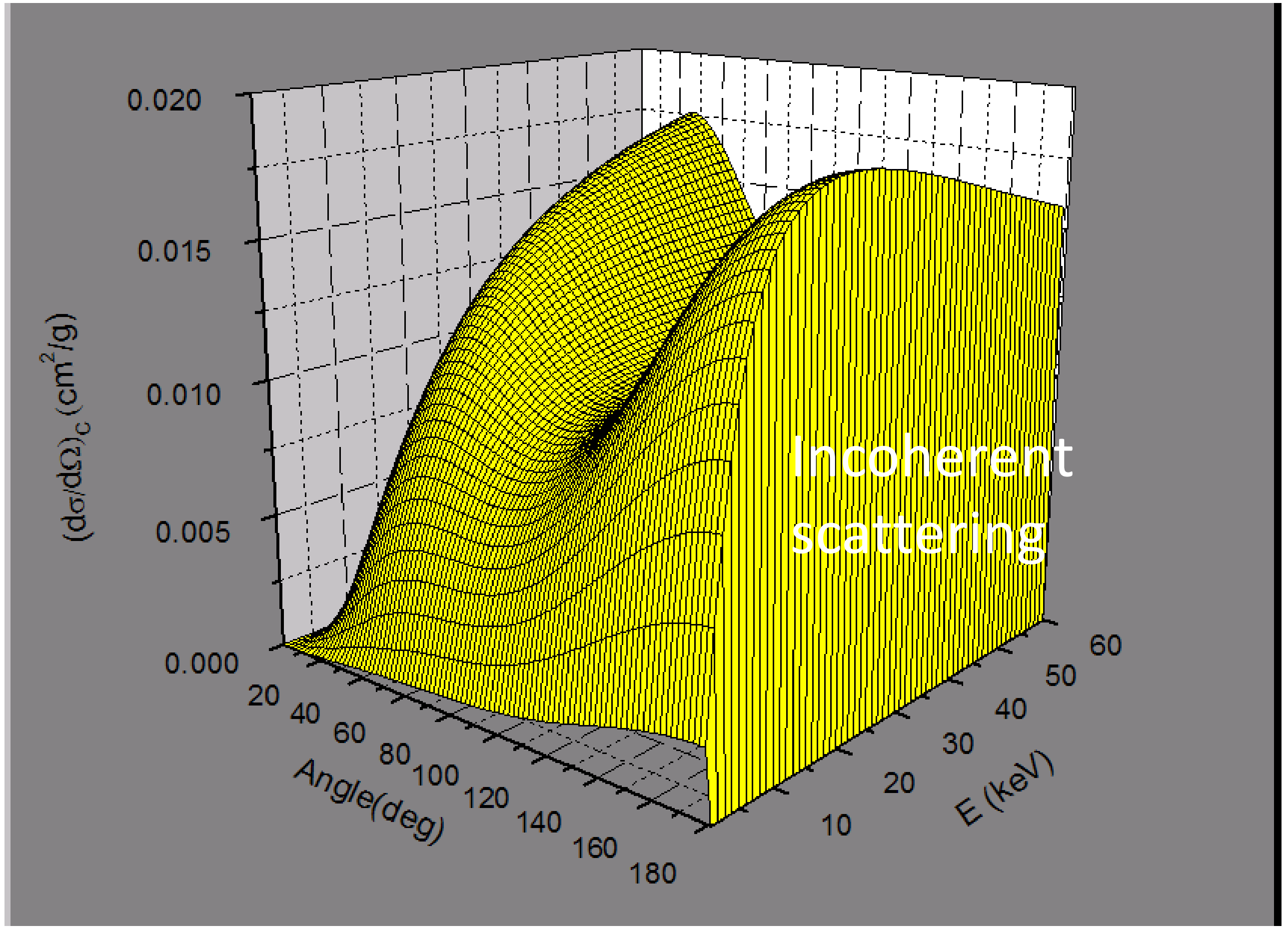

Scattering probabilities: Polarized radiation

Scattering probability ~ $\sin^2\alpha$

α=angle between electric field vector of the incident radiation with the propagation direction of the scattered radiation

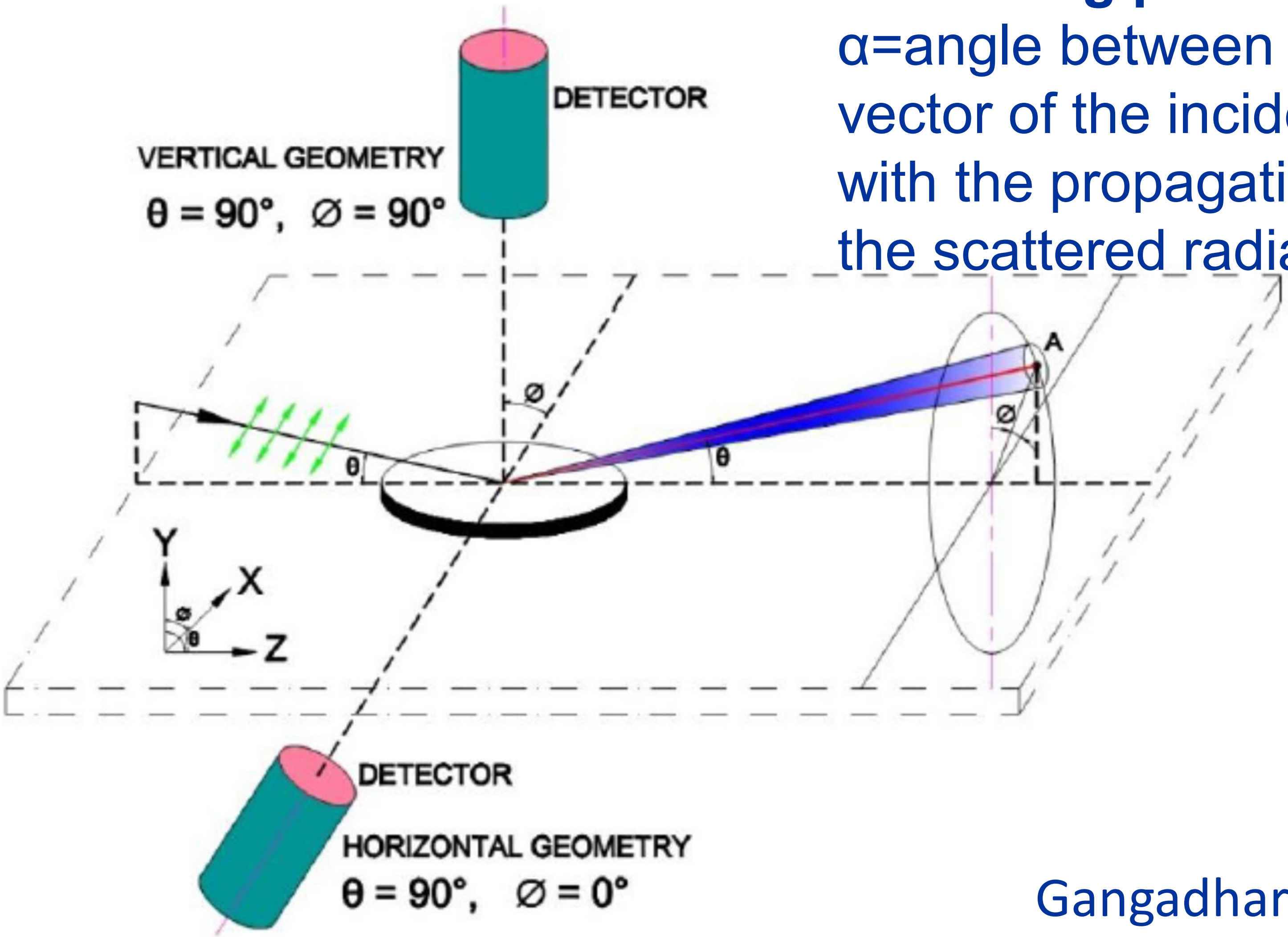

Gangadhar et al. JAAS, 2014

Working principle: X-Ray Fluorescence Analysis

Working principle:

1) Photo-Ionization of **atomic bound electrons** (K, L, M) /**Photoelectric absorption**

2) Electronic transition amd emission of element **'characteristic' fluorescence** radiation

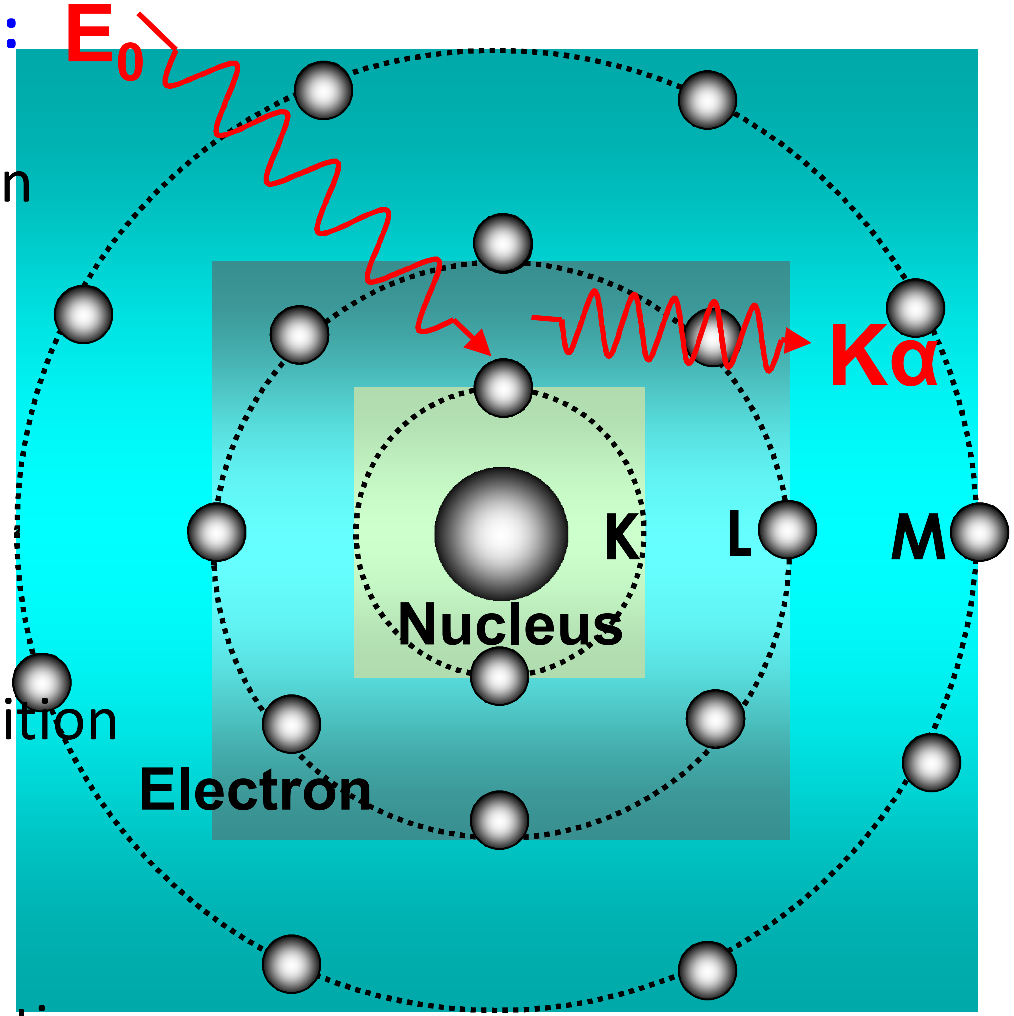

Incident photon Energy E_0 should be adequate to ionize the atomic bound electrons >= Atomic shell Binding energy

De-excitation of atoms: Competitive processes

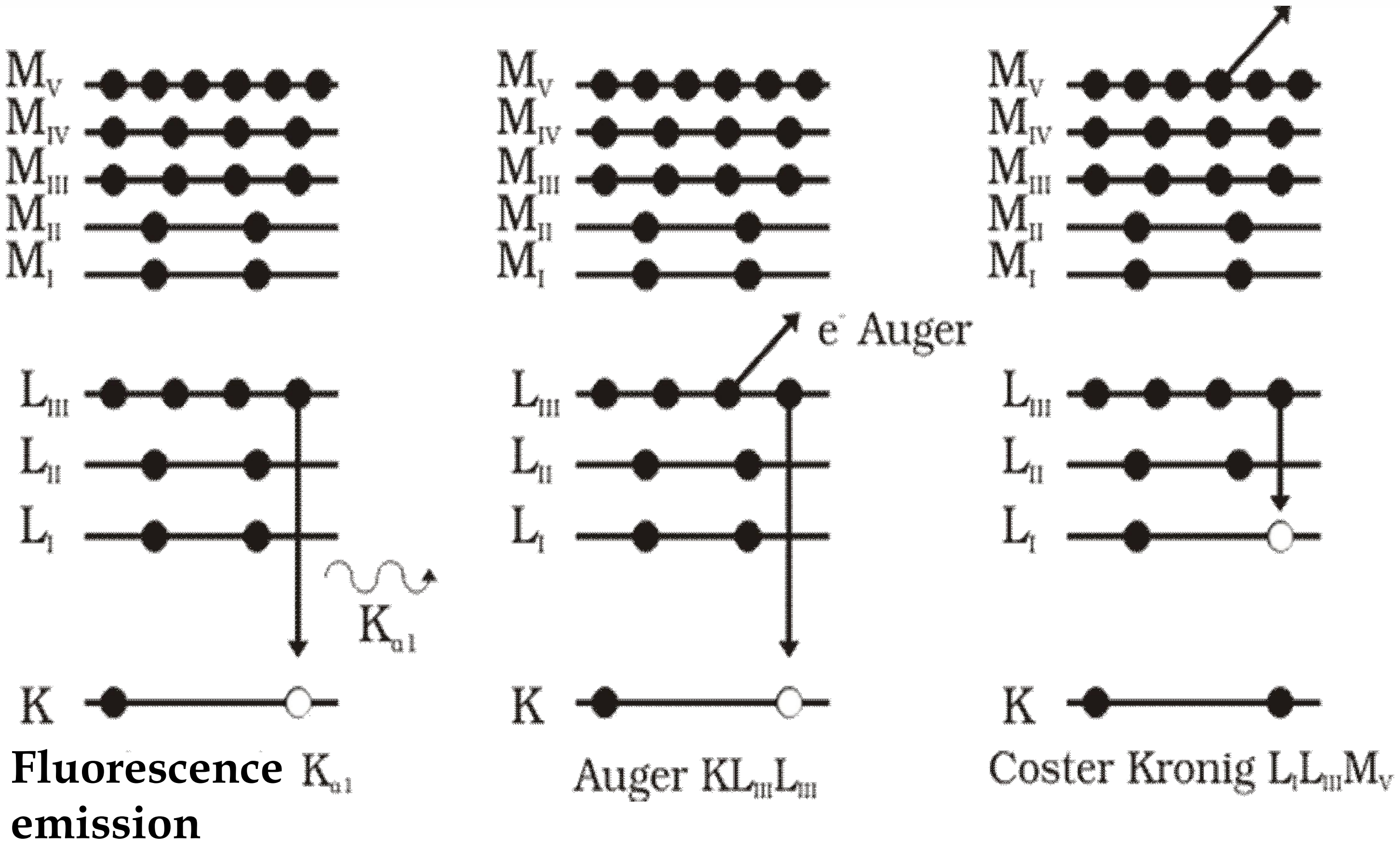

ω_K : K-shell fluorescence yield

f_{Lij} : Coster-Cronig (intra-shell) transition probabilities from the *i* to the *j* L subshell

De-excitation: Fluorescence/Auger yield

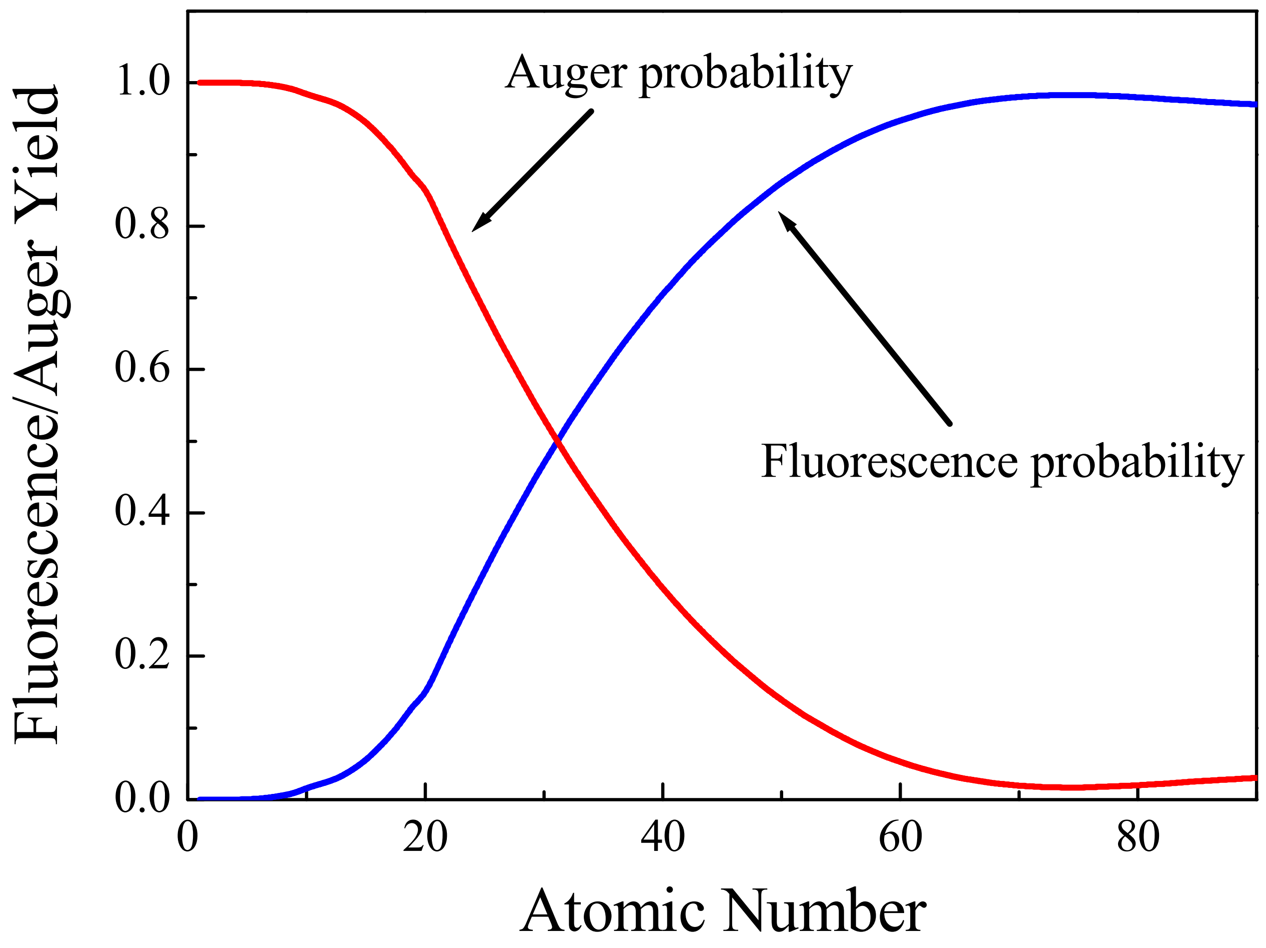

Emission of element ‘characteristic’ x-rays

K - alpha lines: L shell e- transition to fill vacancy in K shell. Most frequent transition, hence most intense peak

K - beta lines: M shell e- transitions to fill vacancy in K shell.

L - alpha lines: M shell e- transition to fill vacancy in L shell.

L - beta lines: N shell e- transition to fill vacancy in L shell.

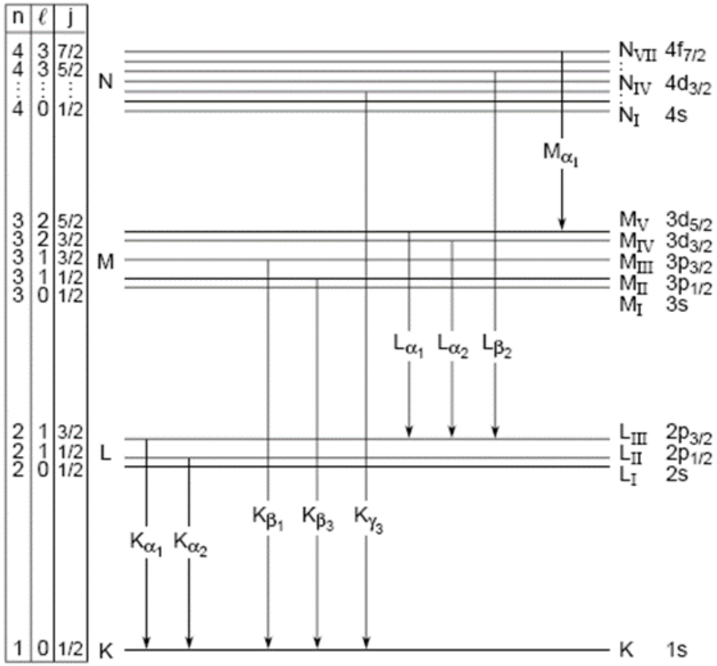

Cu K

$K_{\alpha 1}$: 0.58

$K_{\alpha 2}$: 0.29

$K_{\beta 1}$: 0.08

$K_{\beta 3}$: 0.04

L_3 to K shell → $E_{K\alpha 1} = U_K - U_{L3}$

Each element has a unique set of emission energies

XRF cross sections: K- Emission

XRF K-shell fluorescence cross section, $\sigma_{KX}(E_o)$

$$\sigma_{KX}(E_o) = \tau_K(E_o)\cdot\omega_K\cdot F_{KX}$$

$\tau_K(E_o)$: K-shell photoelectric cross section (*cm²/g or barns/atom*)

ω_K : K-shell fluorescence yield

f_{KX} : Transition probability for Kα emission

XRF cross sections: L- Emission

Example: Incident energy $E_o>U_{L1}$

$$\sigma_{L1X}(E_o)=\tau_{L1}(E_o)\cdot\omega_{L1}(Z_i)\cdot f_{L1X}(Z_i)$$

$$\sigma_{L2X}(E_o)=(\tau_{L2}+\tau_{L1}\cdot f_{L12})\cdot\omega_{L1}(Z_i)\cdot f_{L2X}(Z_i)$$

$$\sigma_{L3X}(E_o)=(\tau_{L3}+\tau_{L2}\cdot f_{L23}\cdot f_{L12}+\tau_{L1}\cdot f_{L13})\cdot\omega_{L3}(Z_i)\cdot f_{L3X}(Z_i)$$

f_{Lij} : Coster-Cronig (intra-shell) transition probabilities from the *i* to the *j* L subshell

XRF cross sections: L- Emission

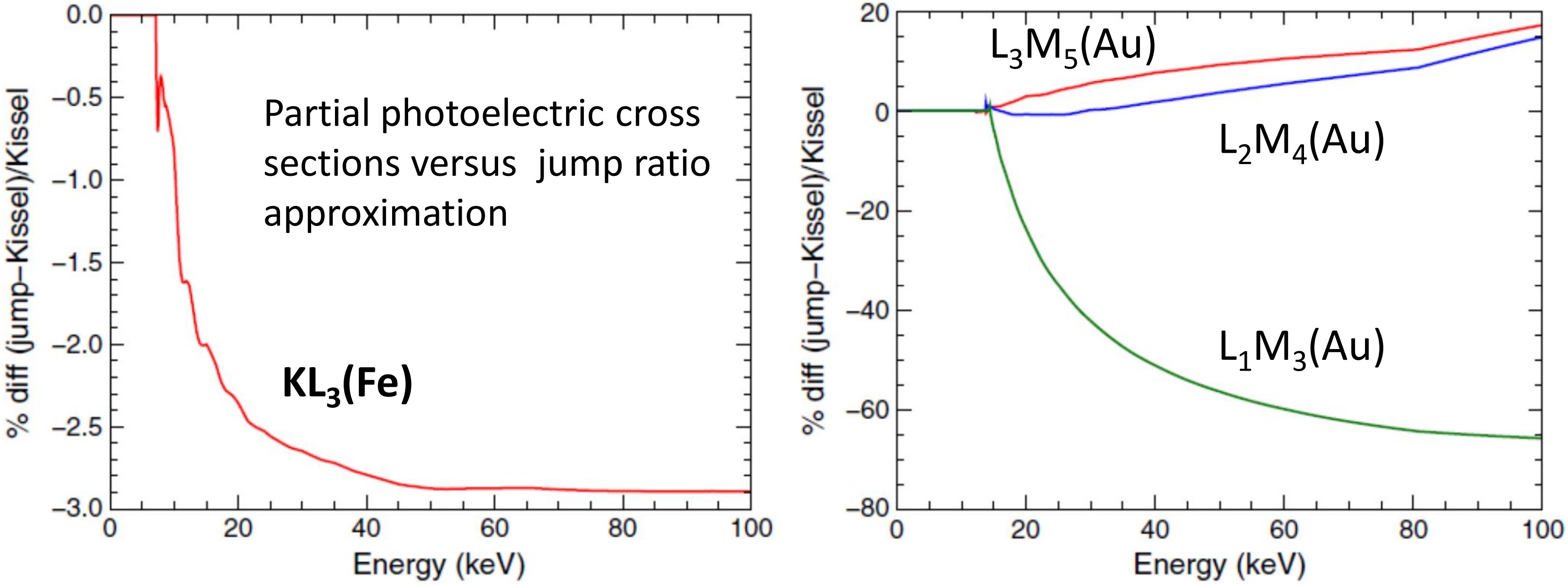

Partial photoelectric cross sections versus jump ratio approximation

XRF cross sections: L- Emission

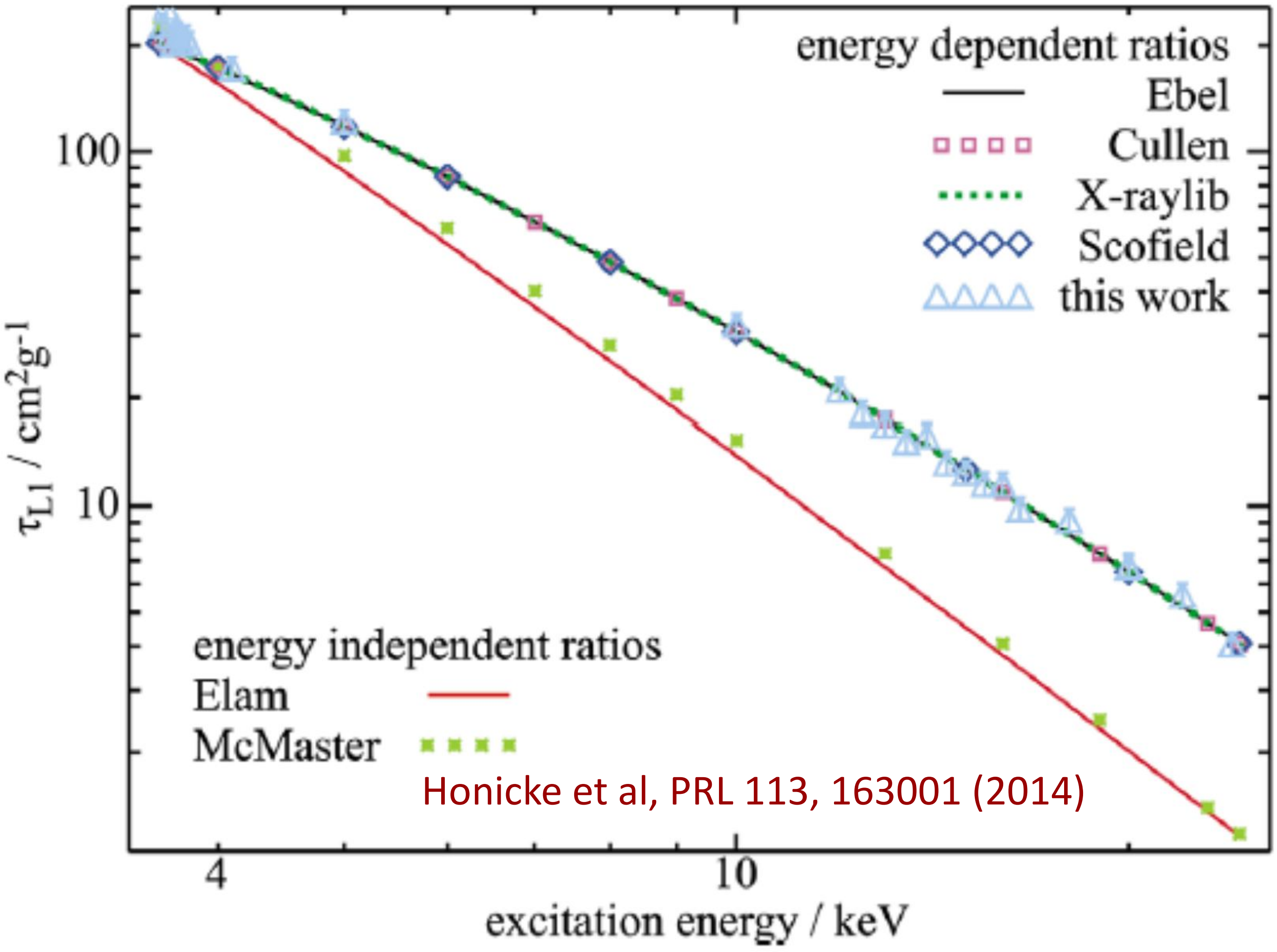

Honicke et al, PRL 113, 163001 (2014)

Fluorescence Kα, Lα cross sections

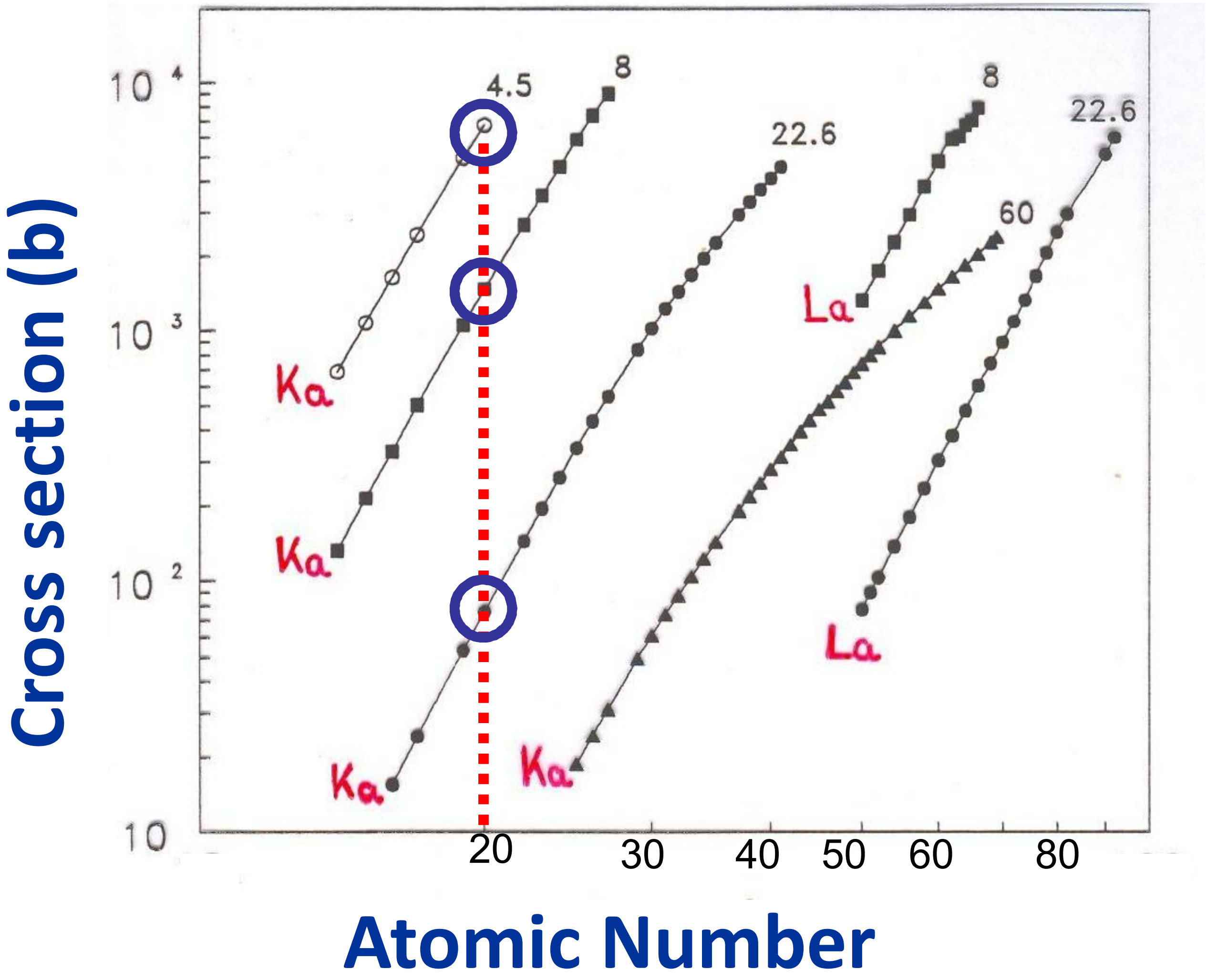

Optimization of the exciting beam energy for maximizing the characteristic X-ray intensity

Primary Fluorescence intensity: Assumptions

- Parallel incident beam
- Infinite surface for sample
- Beam cross section infinite
- Homogenous sample
- Flat surface of the sample

- **D.K.G. de Boer, XRS, 19(1990) 145**
- **M. Mantler, in Handbook of Practical XRFA, Edited by B. Beckhoff et *al*.**

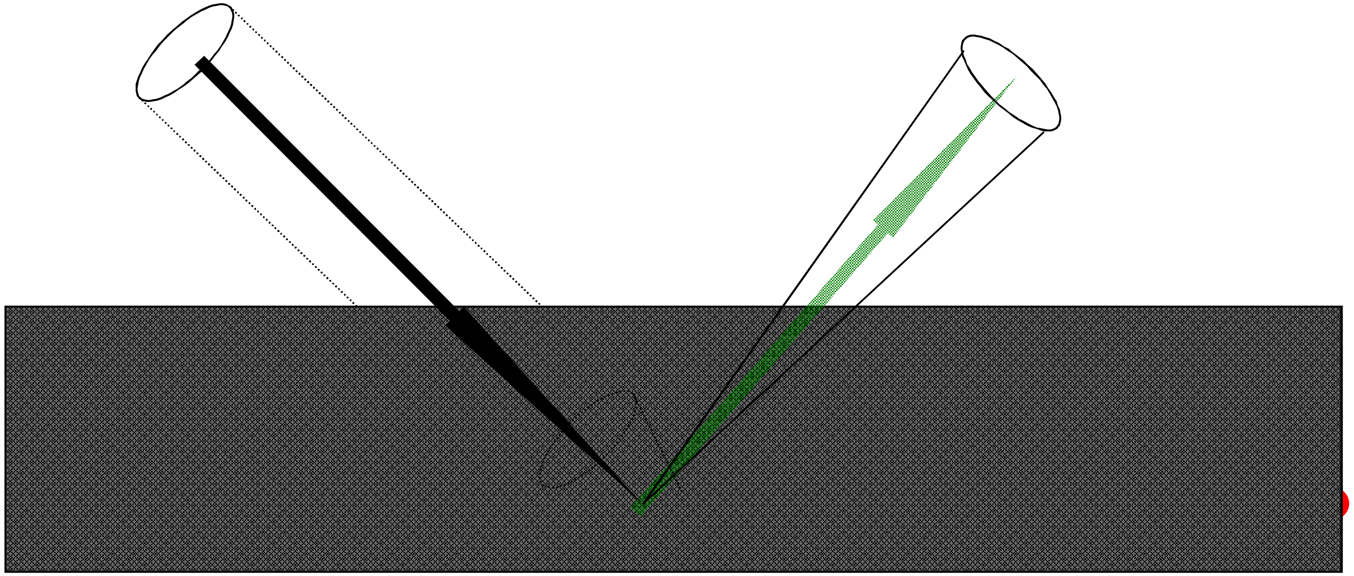

Primary Fluorescence intensity: Assumptions

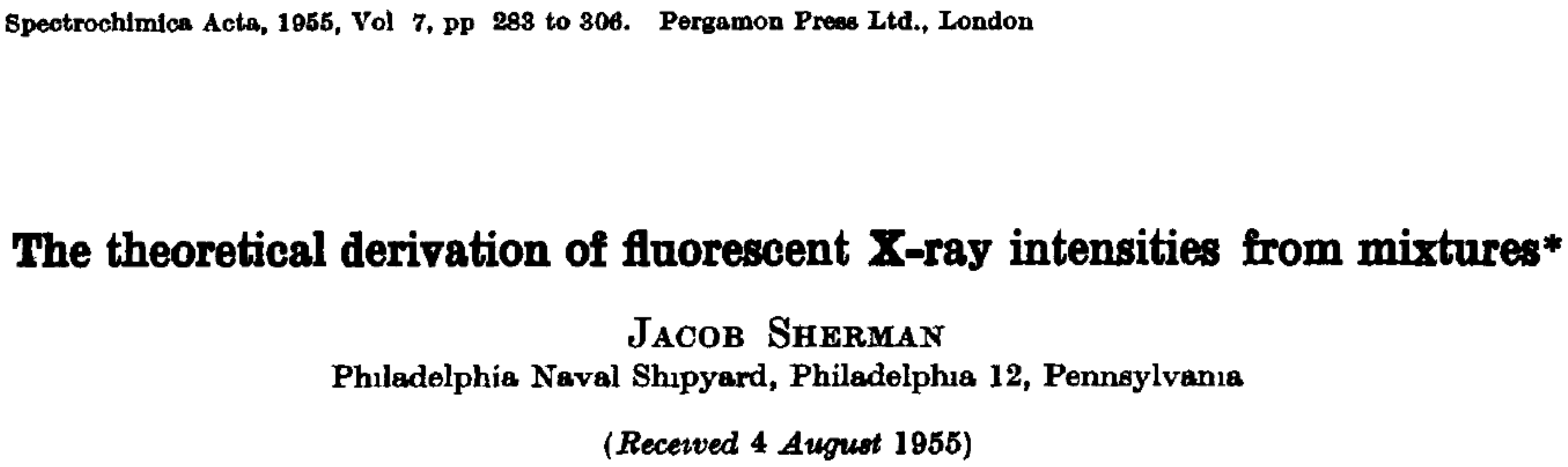

Spectrochimica Acta, 1955, Vol 7, pp 283 to 306. Pergamon Press Ltd., London

The theoretical derivation of fluorescent X-ray intensities from mixtures*

JACOB SHERMAN
Philadelphia Naval Shipyard, Philadelphia 12, Pennsylvania

(*Received* 4 *August* 1955)

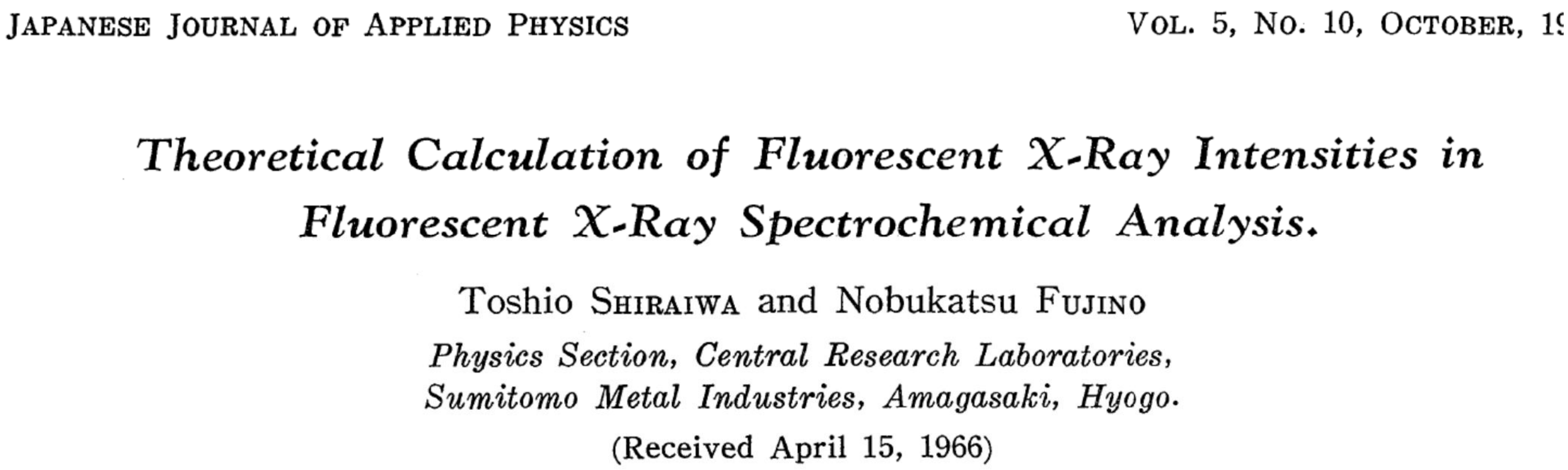

JAPANESE JOURNAL OF APPLIED PHYSICS VOL. 5, NO. 10, OCTOBER, 1

Theoretical Calculation of Fluorescent X-Ray Intensities in Fluorescent X-Ray Spectrochemical Analysis.

Toshio SHIRAIWA and Nobukatsu FUJINO
Physics Section, Central Research Laboratories,
Sumitomo Metal Industries, Amagasaki, Hyogo.

(Received April 15, 1966)

Primary Fluorescence intensity

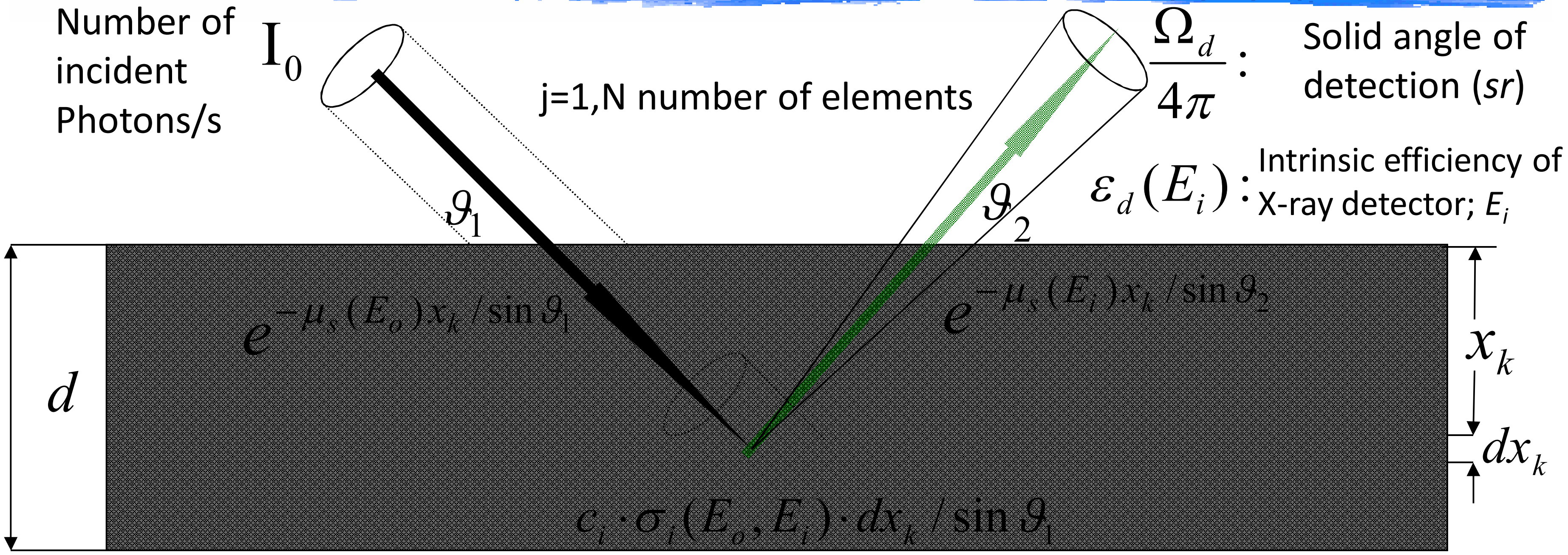

Number of incident Photons/s I_0

j=1,N number of elements

$\frac{\Omega_d}{4\pi}$: Solid angle of detection (*sr*)

$\varepsilon_d(E_i)$: Intrinsic efficiency of X-ray detector; *E*$_i$

(Concentration of *i* element) X (Fluorescence cross section; cm^2/g) X (areal density; g/cm^2)

$\mu_s(E_o)$: Sample mass attenuation coefficient for energy Eo $\equiv \sum_{j=1,N} c_j\mu_j(E_o)$

$$dI_i(E_i) = I_o \cdot e^{-\mu_s(E_o)\cdot x_k/\sin\vartheta_1} c_i \cdot \sigma_i(E_o,E_i)\cdot \frac{dx_k}{\sin\vartheta_1}\cdot e^{-\mu_s(E_i)\cdot x_k/\sin\vartheta_2}\,\frac{\Omega_d}{4\cdot\pi}\cdot\varepsilon_d(E_i)$$

$$\mu_T(E_o,E)_i \equiv \mu_s(E_o)/\sin\vartheta_1 + \mu_s(E_i)/\sin\vartheta_2$$

Primary Fluorescence intensity: Calibration

$I_i(E_i) =$ [redacted] $c_i \cdot \dfrac{1-e^{-\mu_T(E_o,E_i)\cdot d}}{\mu_T(E_o,E_i)} \cdot$ [redacted]

Sensitivity $S_i(E_o, E_i)$

$\mu_T(E_o, E_i) \cdot d \gg 1 \quad I_i(E_i) = S_i(E_o,E_i) \cdot c_i \cdot \dfrac{1}{\mu_T(E_o,E_i)}$ Thick target approximation

$\mu_T(E_o, E_i) \cdot d \ll 1 \quad I_i(E_i) = S_i(E_o,E_i) \cdot c_i \cdot d$ Thin target

Different approaches are followed depending on how well the set-up geometry and incident beam intensity are characterized:

- **Sensitivity calibration:** certified pure element/compound targets
- **Solid angle calibration:** Normalized beam intensity, detector efficiency known, well certified pure element/compound targets
- **Standard-less XRFA:** Calibrated apertures, distances, detector response function versus energy, incident beam intensity

Indirect Enhancement Processes in Fluorescence Emission

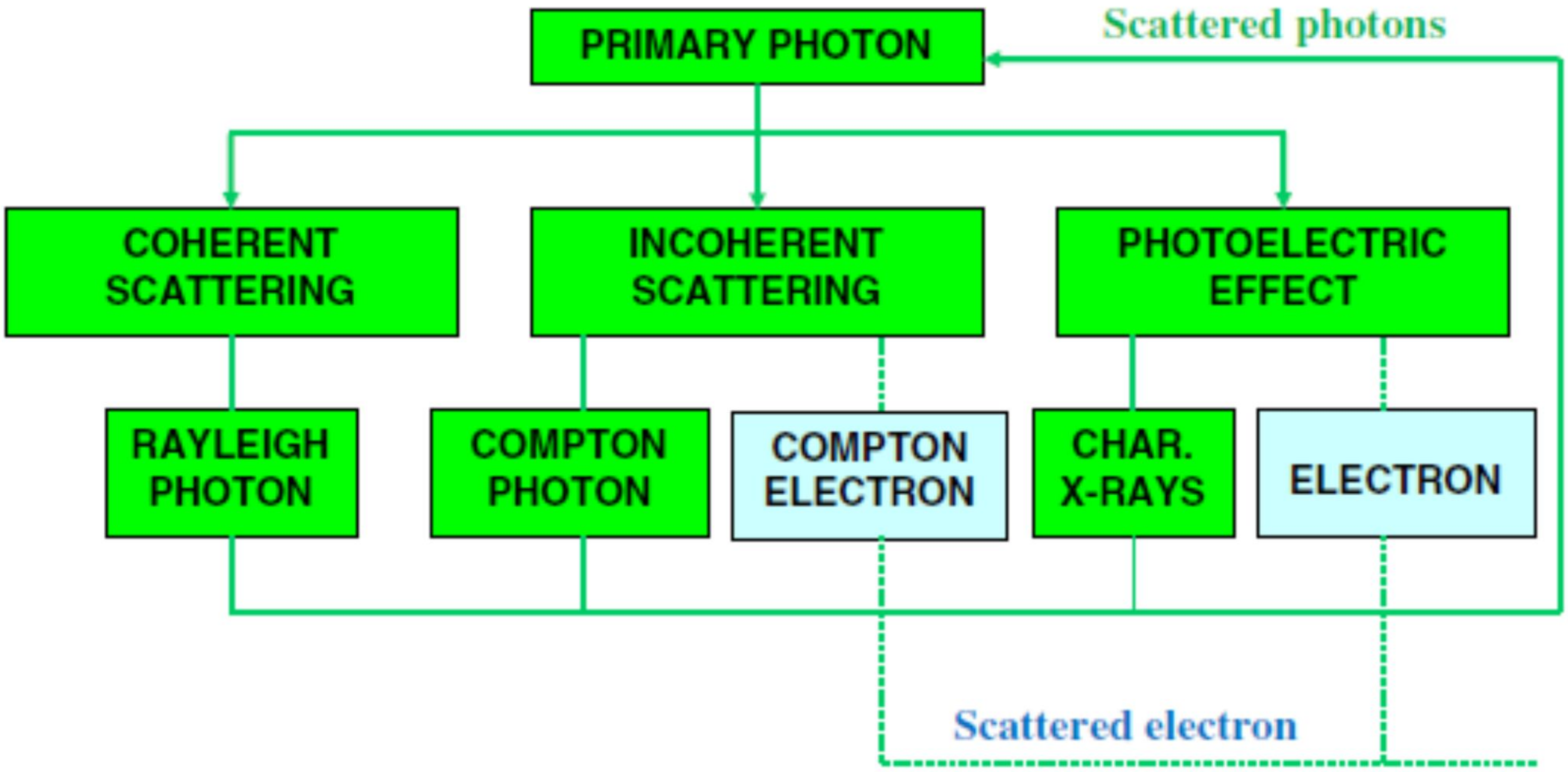

J. Fernandez et *al*., X-Ray Spectrom. 2013, 42, 189–196

Indirect Enhancement Processes in Fluorescence Emission

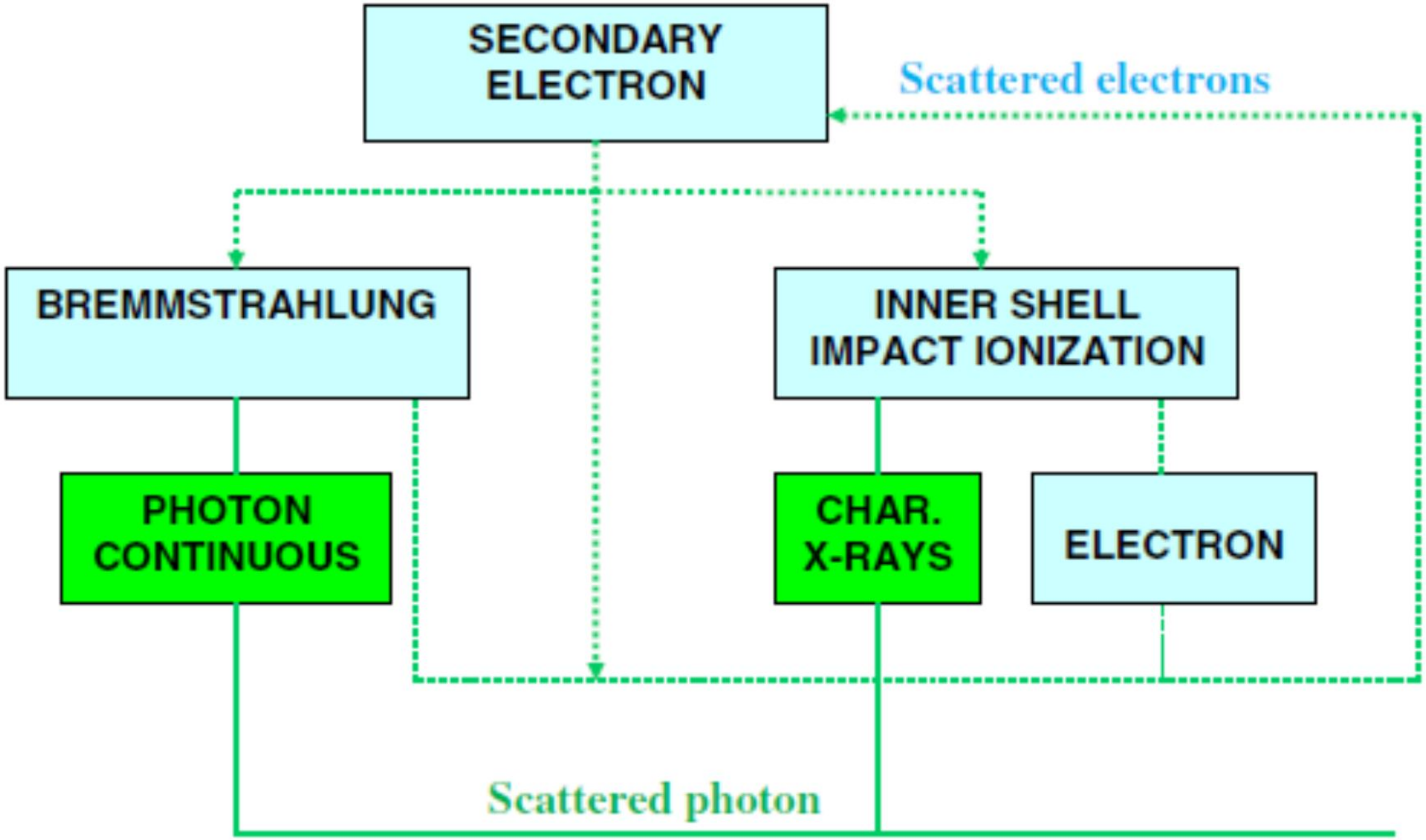

SECONDARY ELECTRON

BREMMSTRAHLUNG

INNER SHELL IMPACT IONIZATION

PHOTON CONTINUOUS

CHAR. X-RAYS

ELECTRON

Scattered electrons

Scattered photon

J. Fernandez et *al*., X-Ray Spectrom. 2013, 42, 189–196

Secondary Fluorescence Enhancement

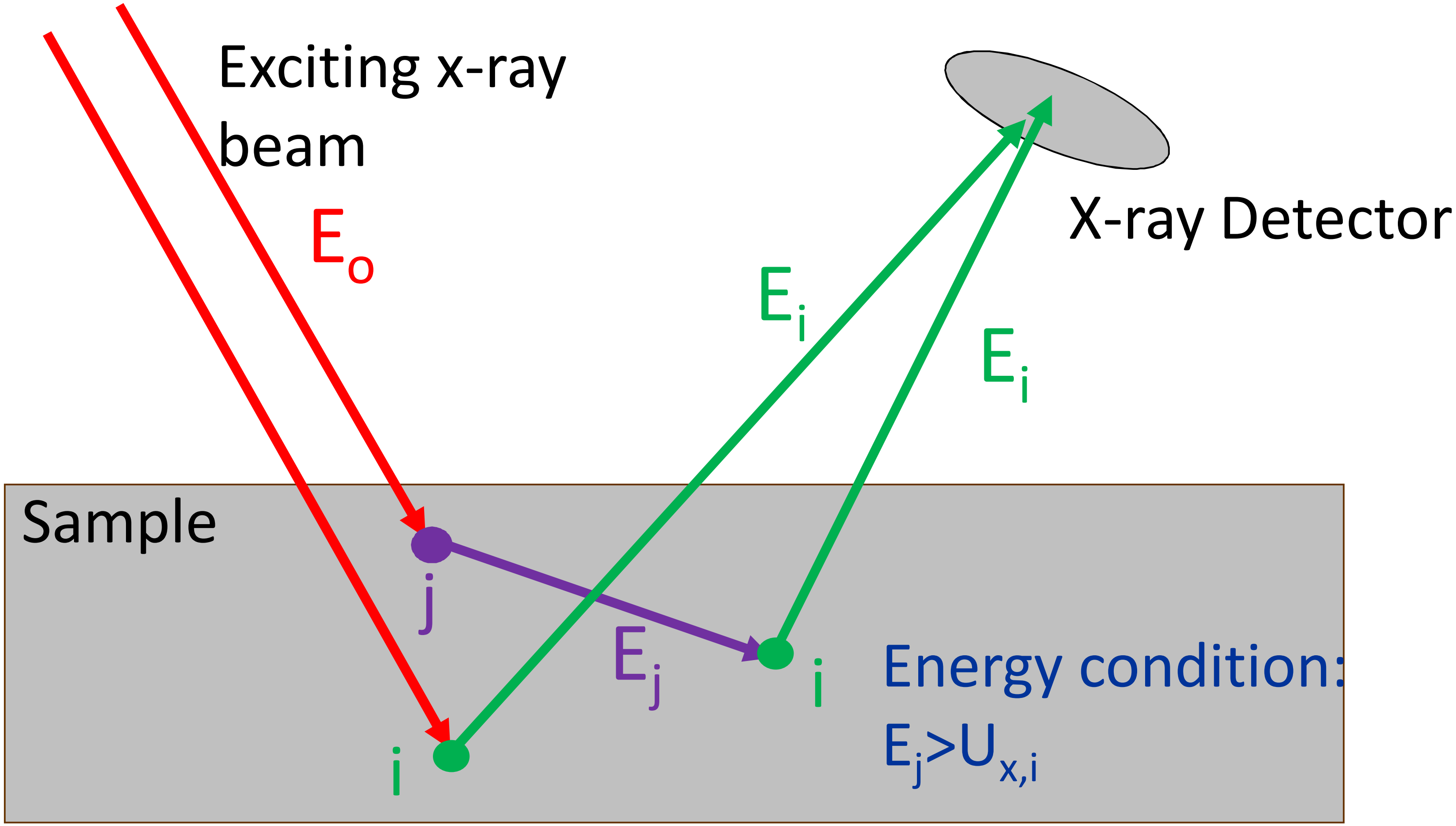

Energy condition:
$E_j > U_{x,i}$

Element ***j*** characteristic x-ray(s) can excite element ***i*** characteristic x-rays within the sample volume

Secondary enhancement calculation: Example

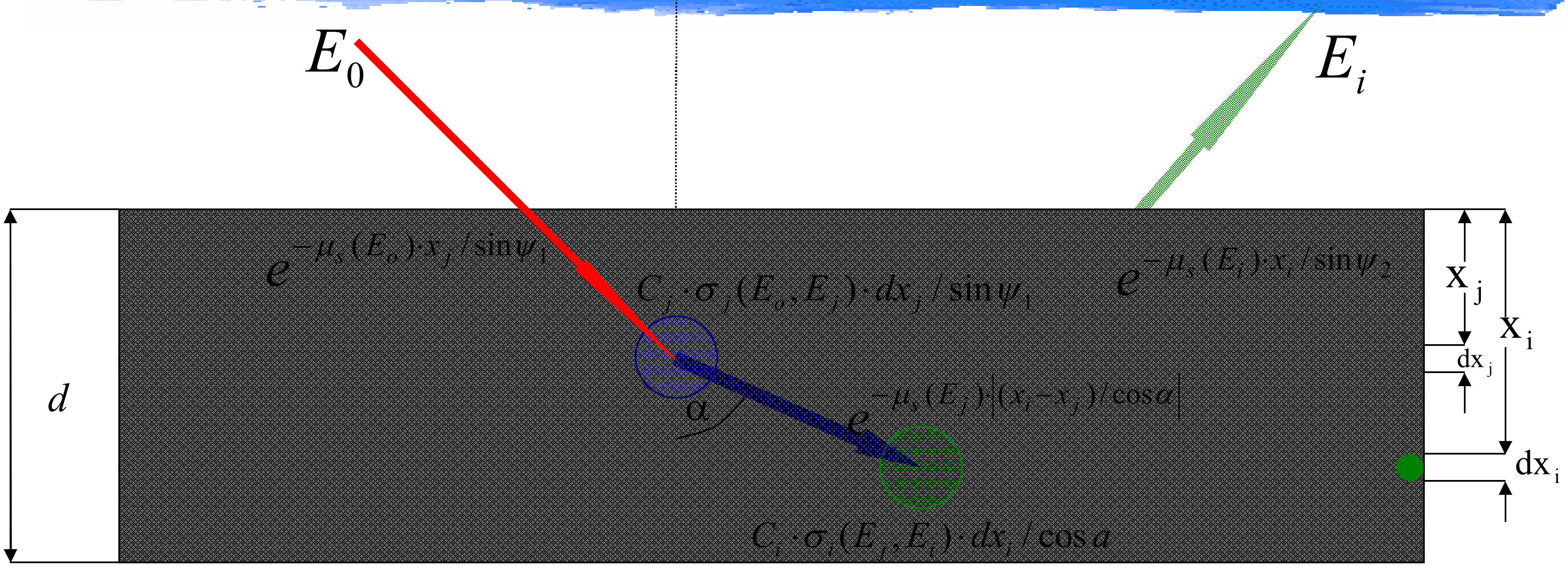

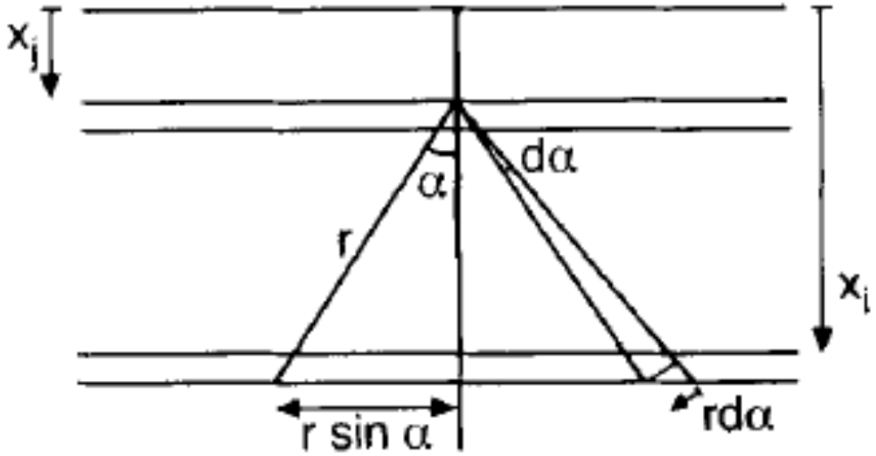

Number of photons emitted per unit area of layer dx_j that reach layer dx_i within the cones with aperture angles *α, α+dα*

$$(2\cdot\pi\cdot r\cdot\sin\alpha)\cdot(r\cdot d\alpha)\times\frac{1}{4\cdot\pi\cdot r^2}=$$

$$\frac{1}{2}\cdot\sin\alpha\cdot d\alpha$$

Topology of secondary fluorescence

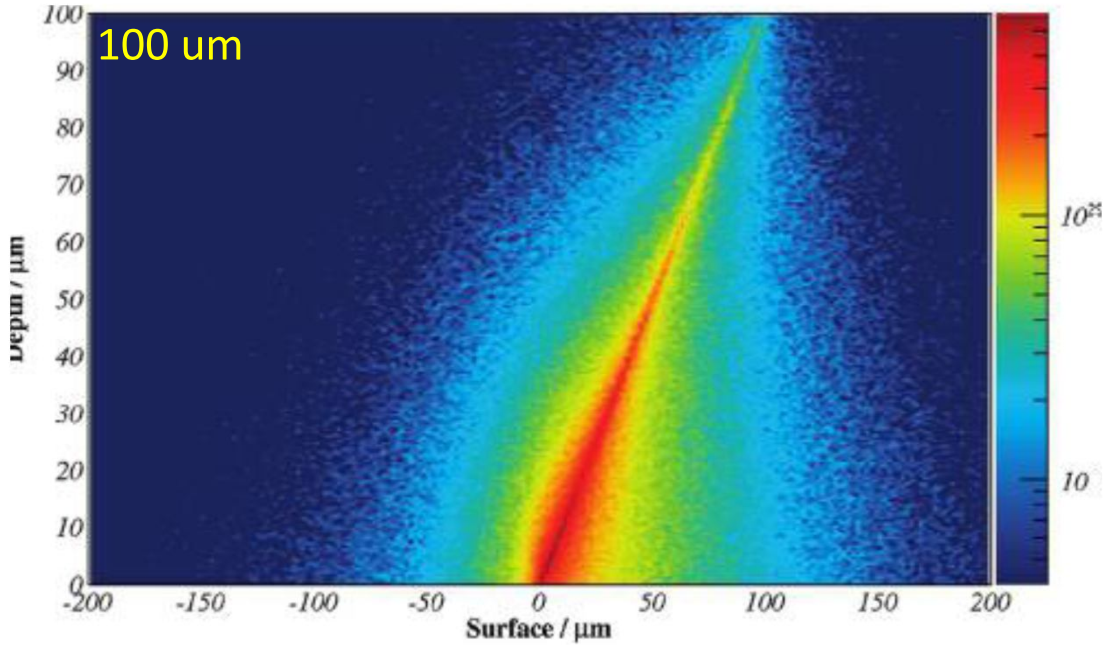

13 keV, excitation, SiO_2 matrix, 5% Cu, 5% Fe

Sokaras et al, Anal. Chem. 2009, 81, 4946

Tertiary Fluorescence Enhancement

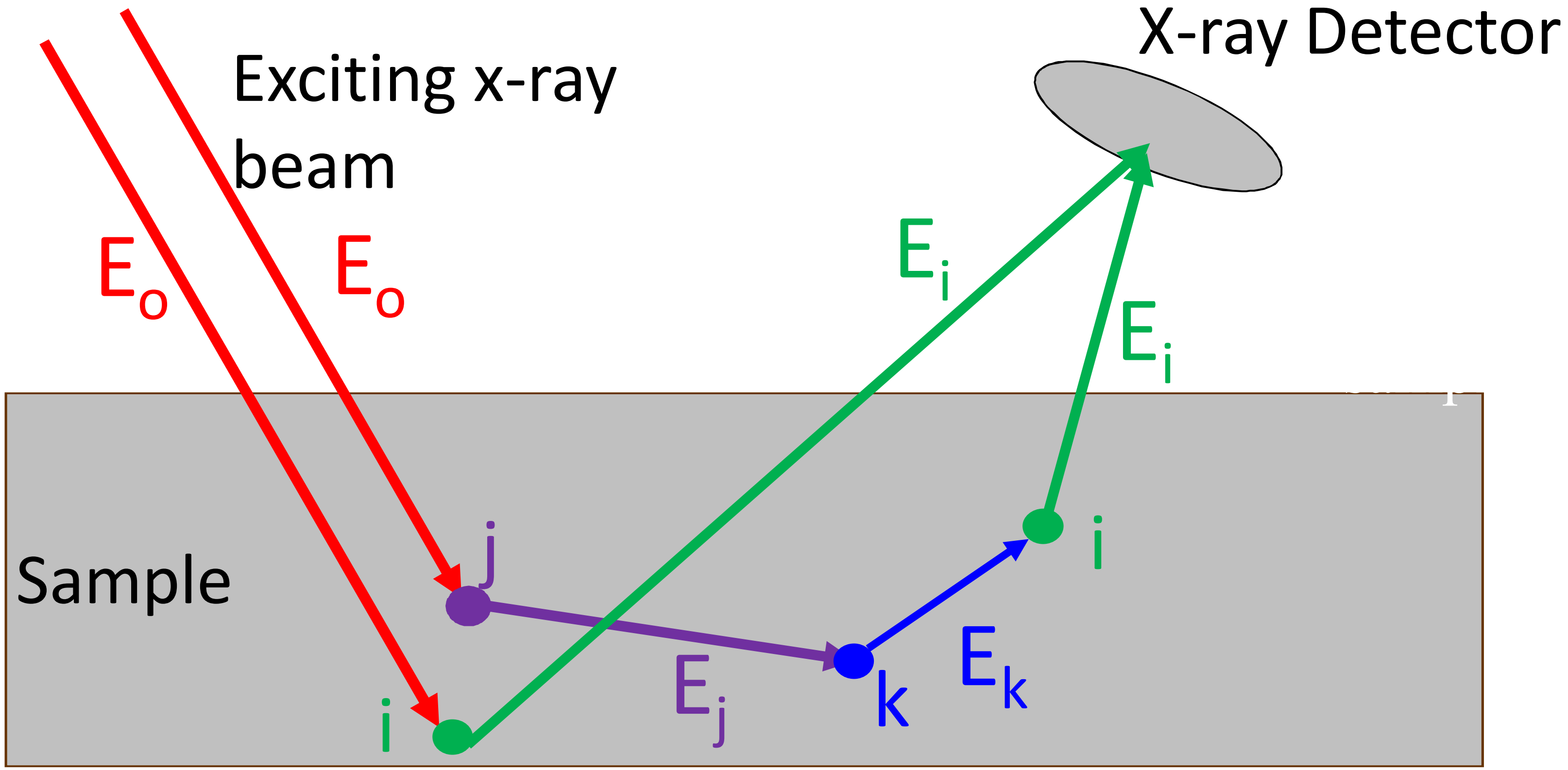

The element ***j*** characteristic x-ray(s) can excite element’s ***k*** characteristic x-ray(s) which consequently can also excite element’s ***i*** characteristic x-rays

Energy conditions:$E_j > U_{x,k}$ and $E_k > U_{x,i}$

SF Enhancement in Poly-Energetic excitation

Type of Sample	Secondary Fluorescence Mechanism	Am-241 (59.6 keV) Source*	Filtered Rh-tube excitation*
Ag: 92.5% Cu: 7.5 %	Ag-K to Cu	1.57	0.29
Au: 88.3 % Ag: 8.5 % Cu: 3.1 %	(Ag-K+Au-L) to Cu	0.82	0.55
	Ag-K to Au	6.6e-2	1.4e-2
Cu: 80 % Pb: 10 % Sn: 10 %	(Sn-K + Pb-L) to Cu	0.22	7.8e-2
	Sn-K to Pb	0.11	1.6e-2

* Including ternary contribution

Self-element SF Enhancement (special case)

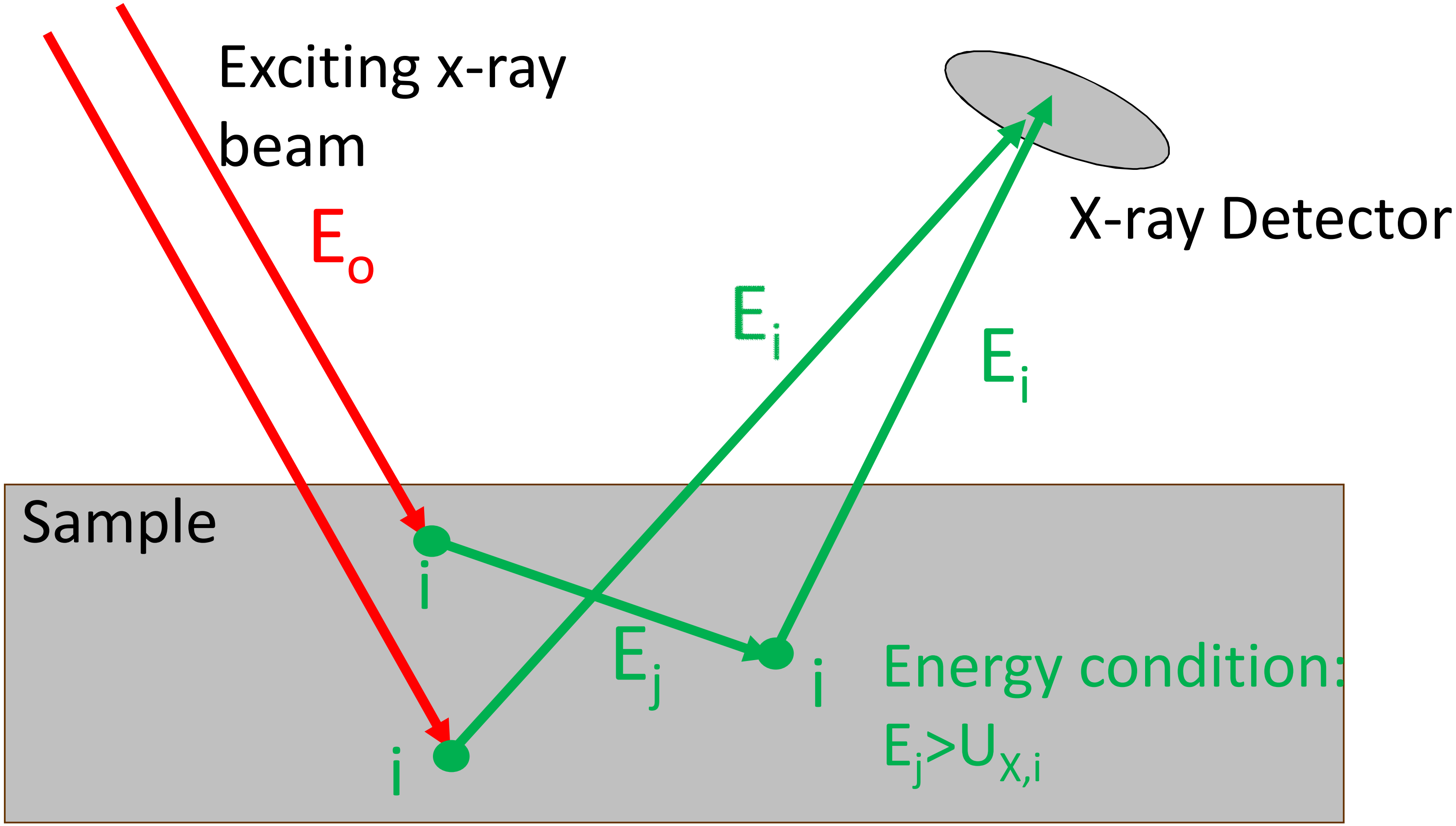

Element ***i*** characteristic x-ray(s) can excite different series of characteristic X-rays of the same element ***i*** within the sample volume; for example K to L, L to M lines

Self-element SF Enhancement (special case)

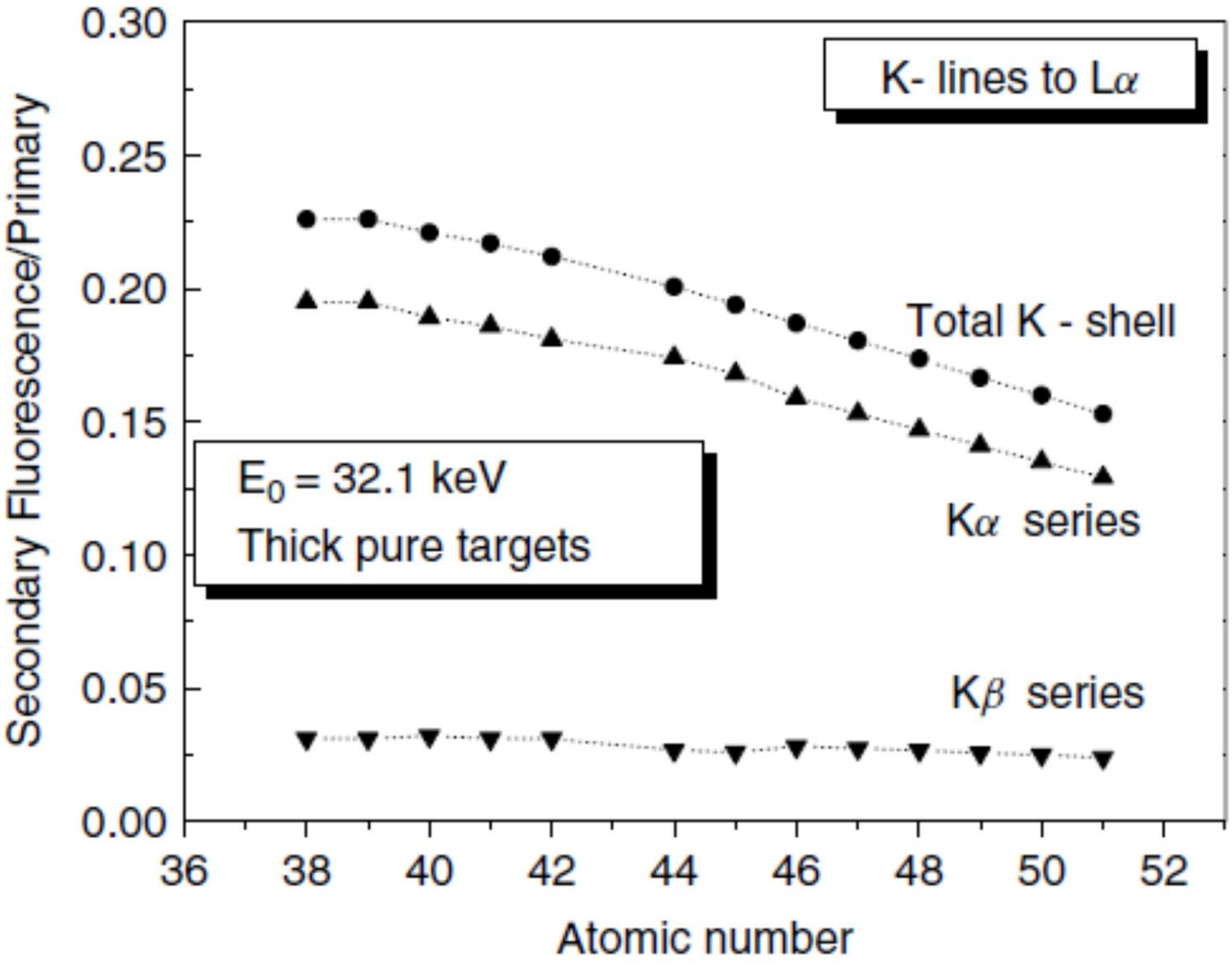

A.G. Karydas et al., X-Ray Spectrom. 2005; 34: 426–431

Self-element SF Enhancement (special case)

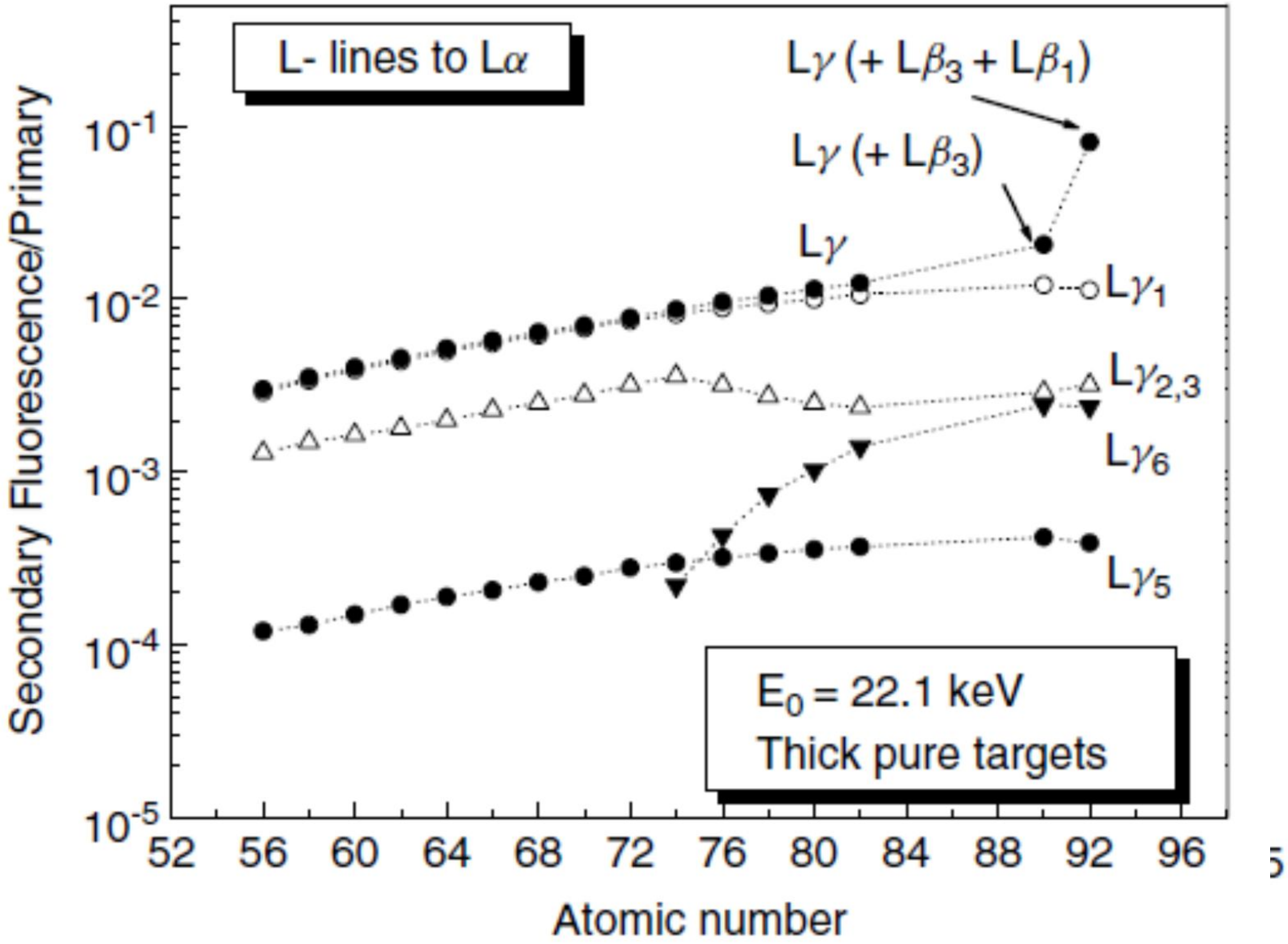

A.G. Karydas et al., X-Ray Spectrom. 2005; 34: 426–431

Self-element SF Enhancement (special case)

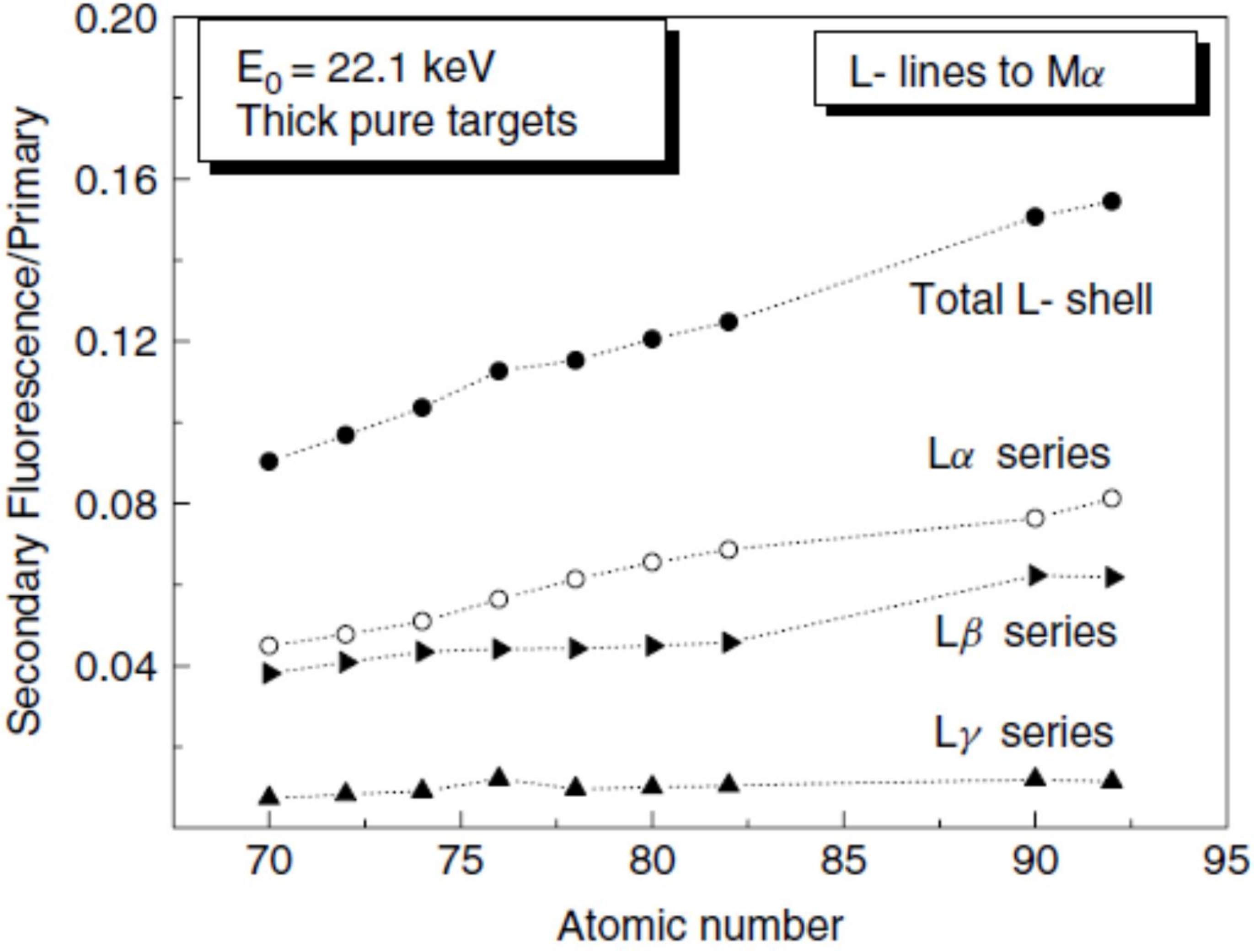

A.G. Karydas et al., X-Ray Spectrom. 2005; 34: 426–431

Secondary Scattering Enhancement (Beam)

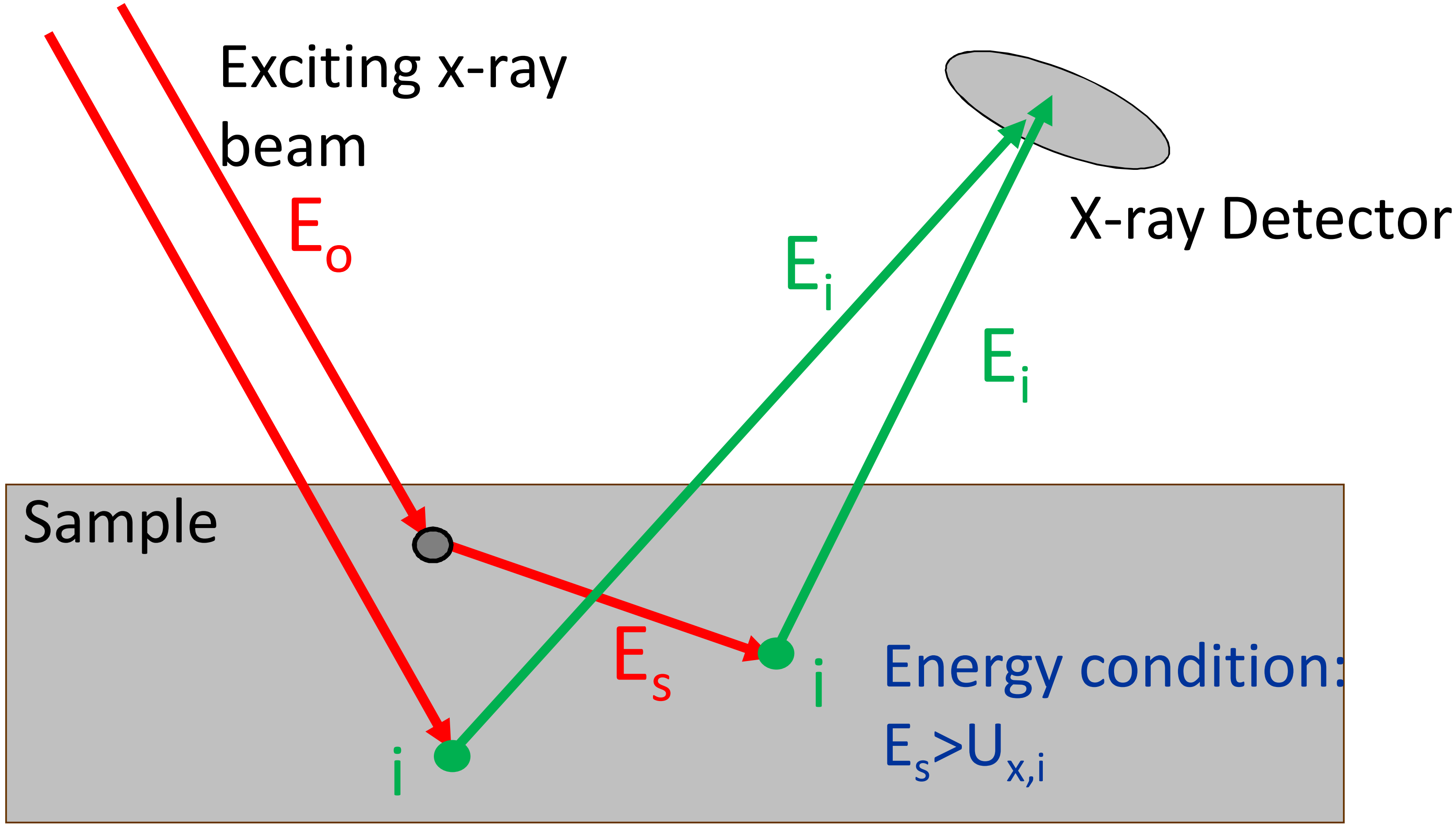

Energy condition:

$E_s > U_{x,i}$

Incident beam after encountering elastic/inelastic scattering at one produces photoionization of an element *i* in another sample position volume

Secondary Scattering Enhancement (Fluo)

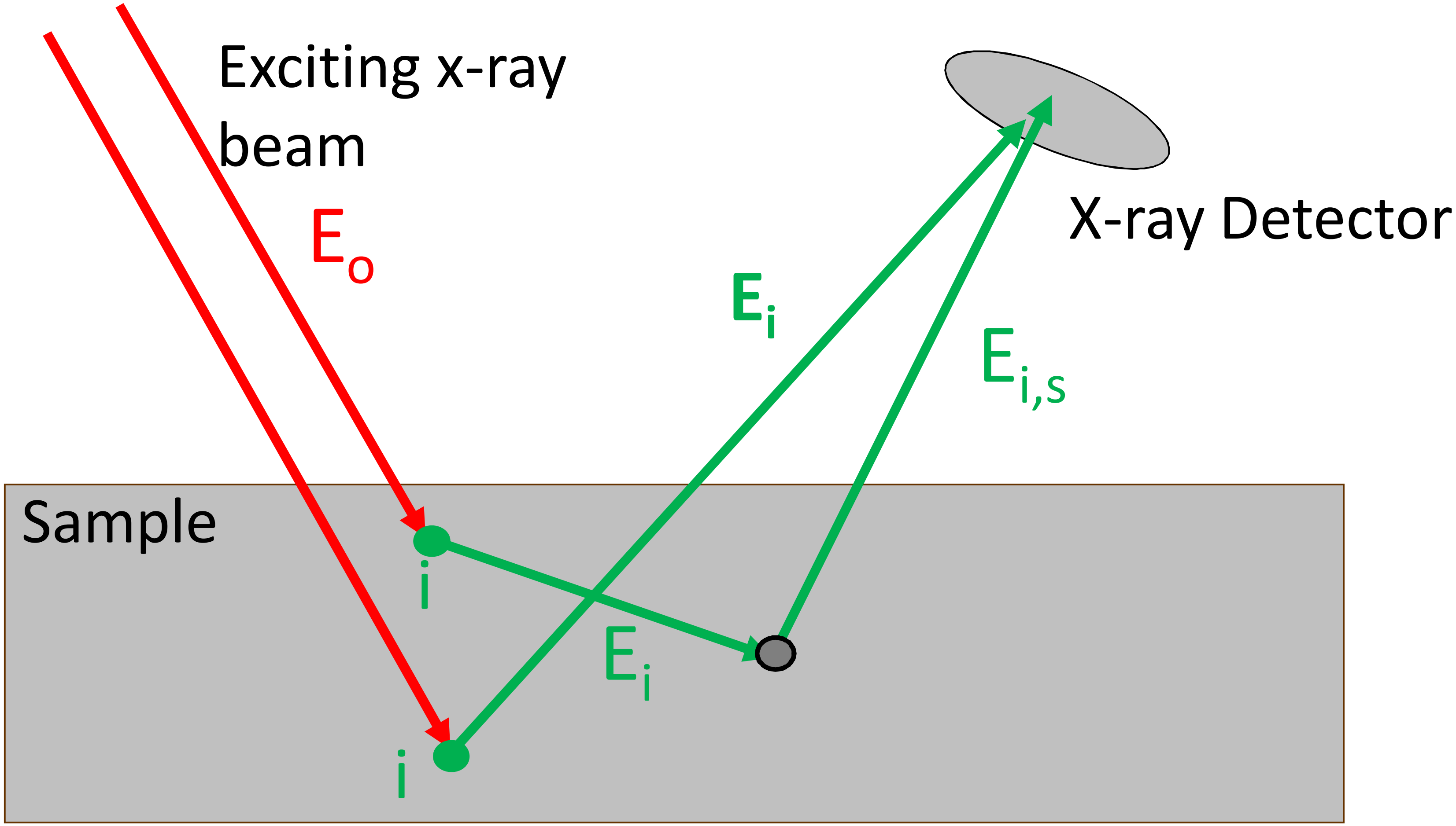

Element a characteristic x-ray after elastic/inelastic scattering within the sample volume are directed to the detector

Secondary Enhancement due to Scattering

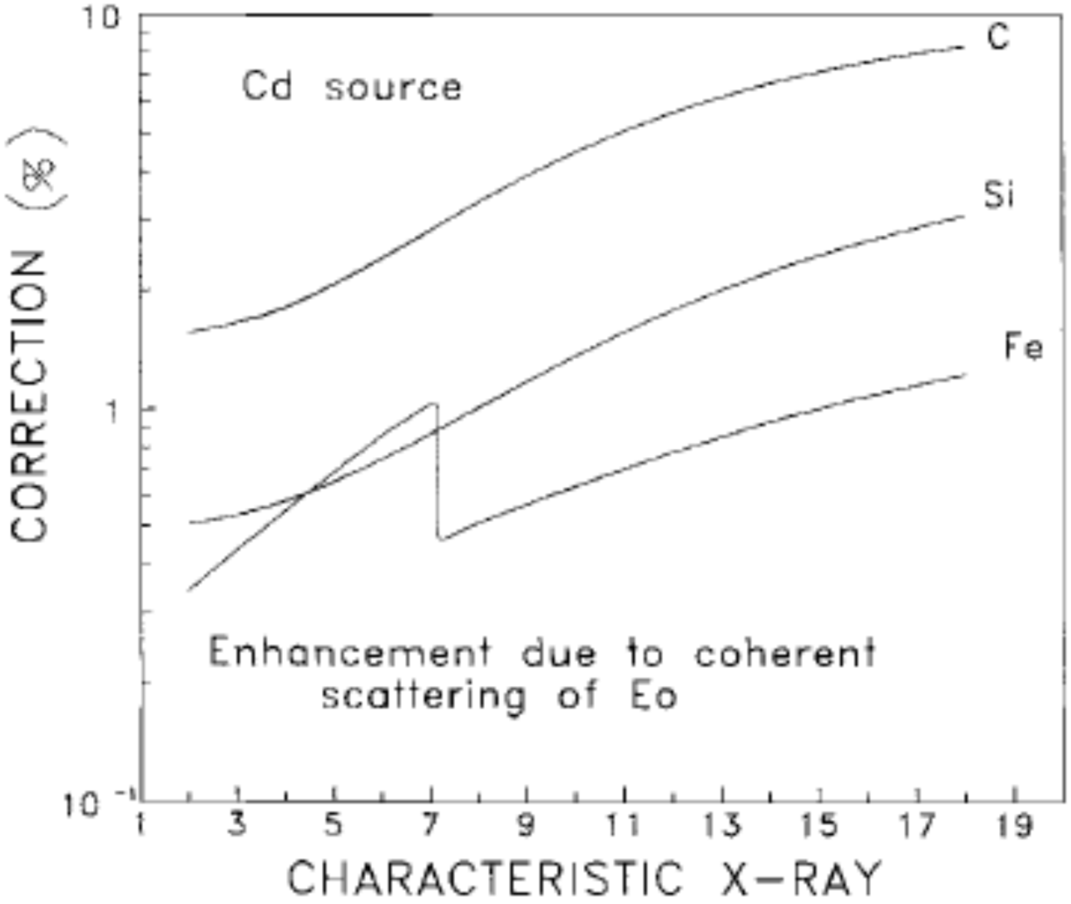

Karydas, Paradellis, X-Ray Spectrom. 1993; 22: 208
Tirao, Stutz, X-Ray Spectrom. 2003; 32: 13–24

Secondary Enhancement due to Scattering

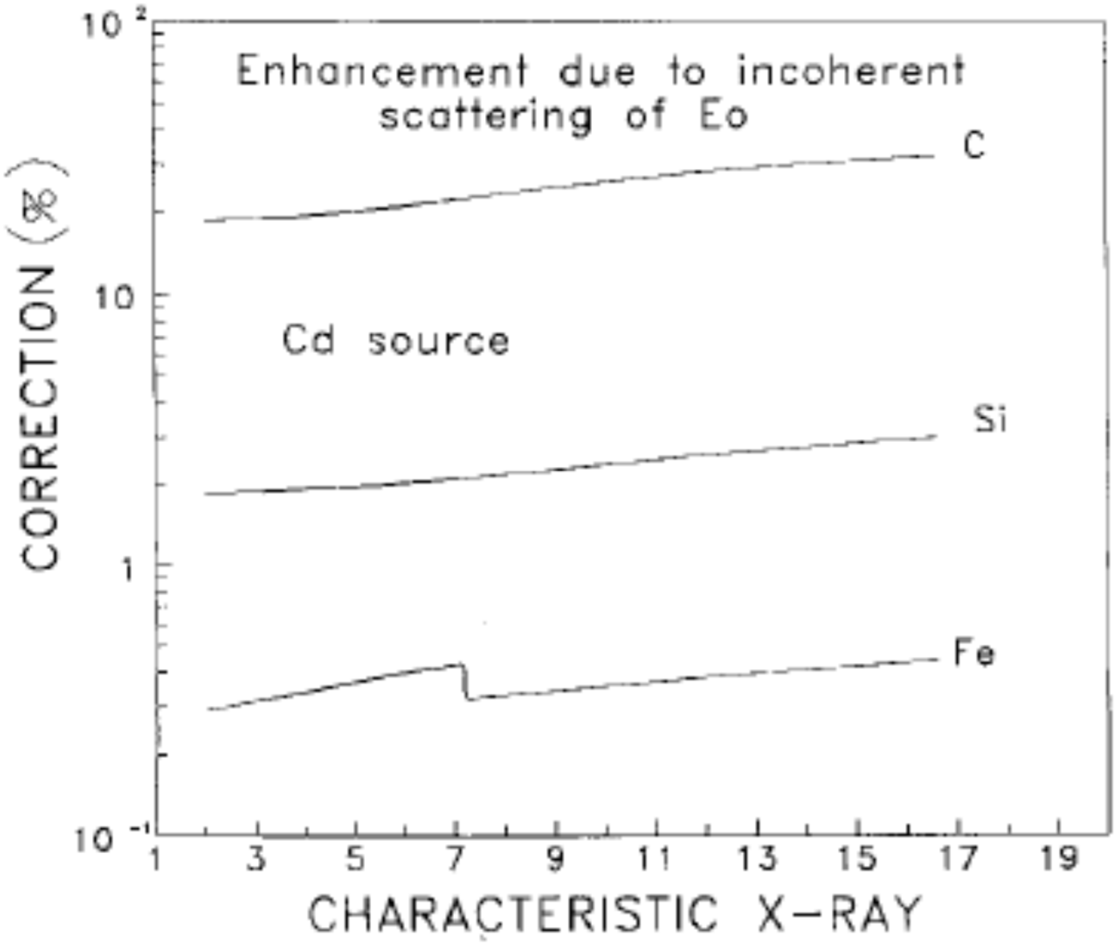

Karydas, Paradellis, X-Ray Spectrom. 1993; 22: 208

Tirao, Stutz, X-Ray Spectrom. 2003; 32: 13–24

Secondary Enhancement due to Scattering

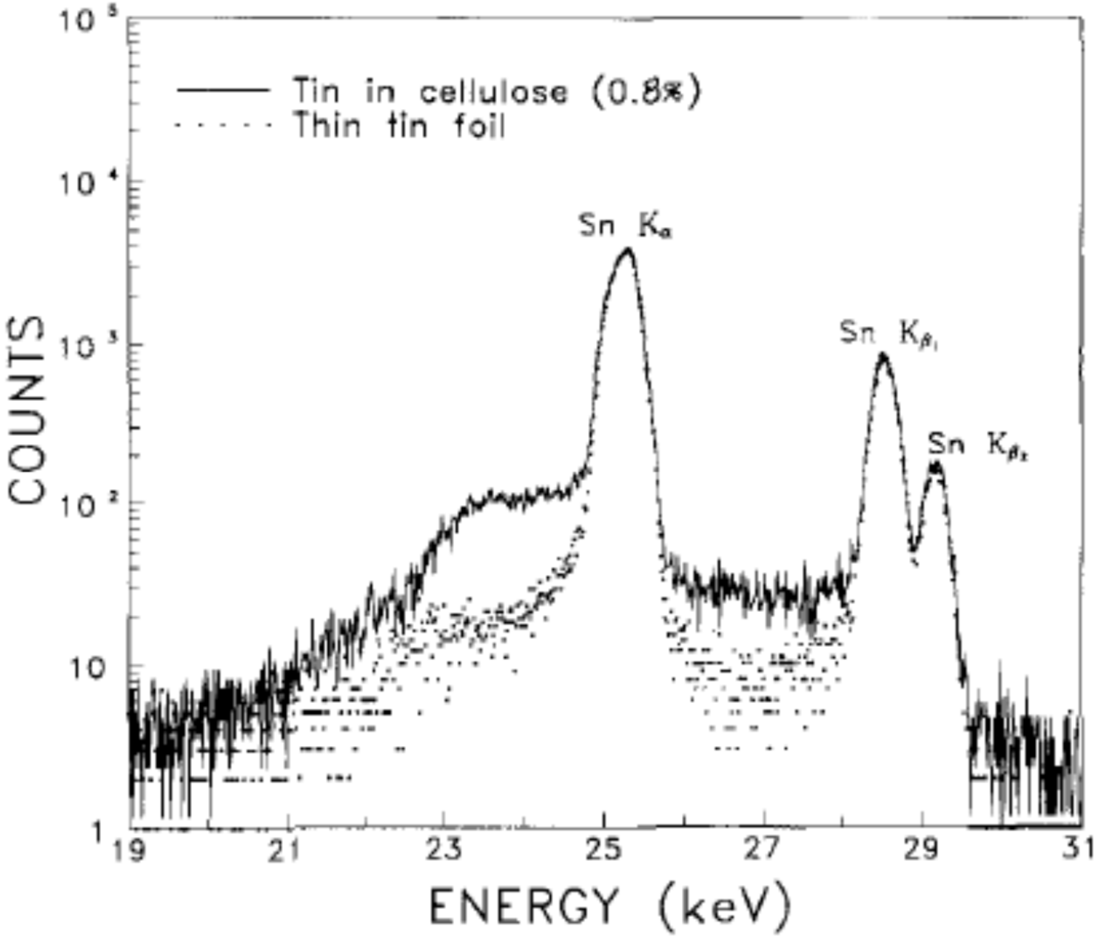

Effect on spectrum!

Karydas, Paradellis, X-Ray Spectrom. 1993; 22: 208
Tirao, Stutz, X-Ray Spectrom. 2003; 32: 13–24

Photo-/Auger/Compton e⁻ Indirect Fluorescence Enhancement

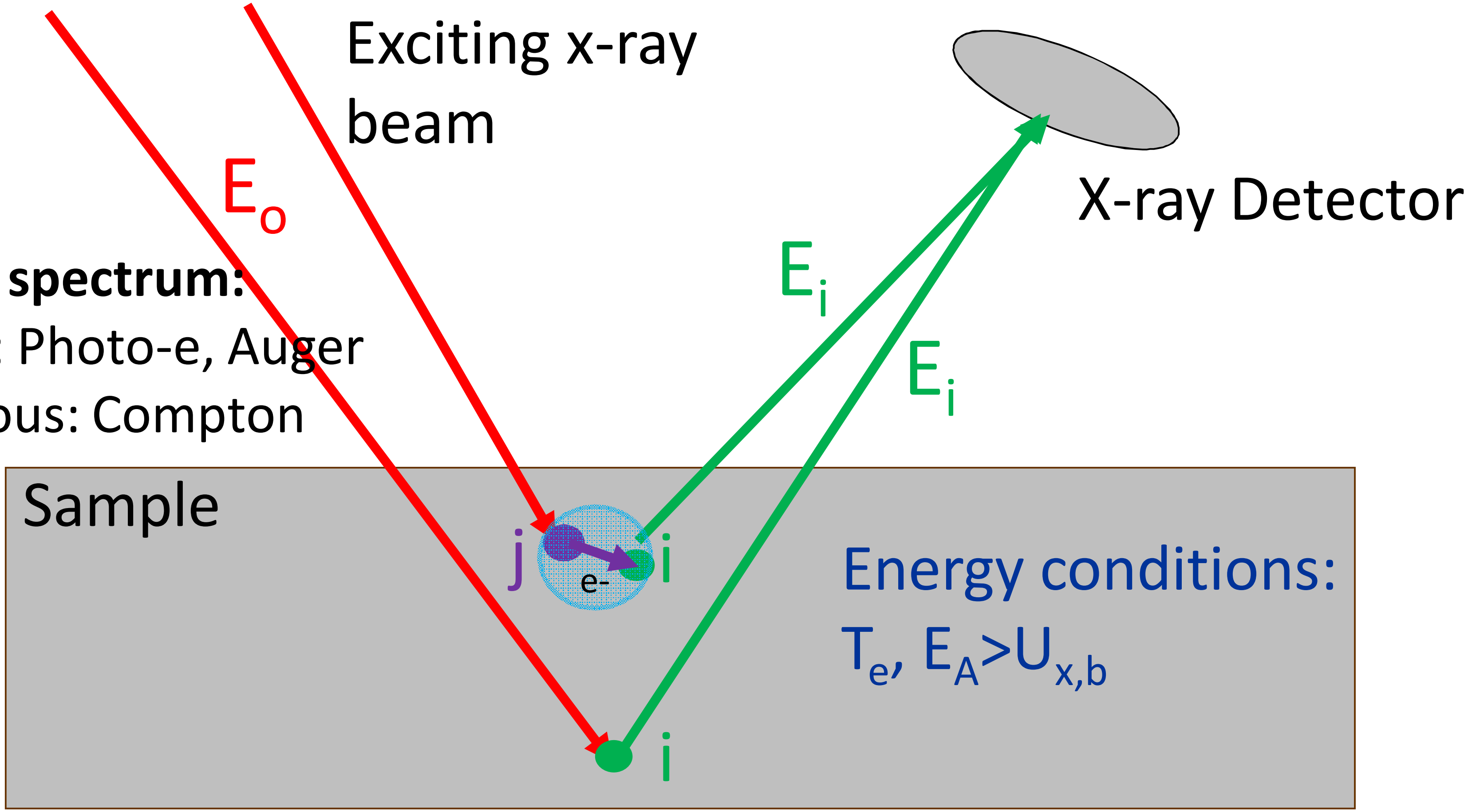

Electron spectrum:
Discrete: Photo-e, Auger
Continuous: Compton

Energy conditions:
T_e, $E_A > U_{x,b}$

Ejected electrons from the atoms of element ***j*** can ionize an inner shell of element ***i***

Ionization induced by electrons

G
o
e

Q
se
fu
d
c

L
o

Stochastic movement of electrons (20 keV on Fe)

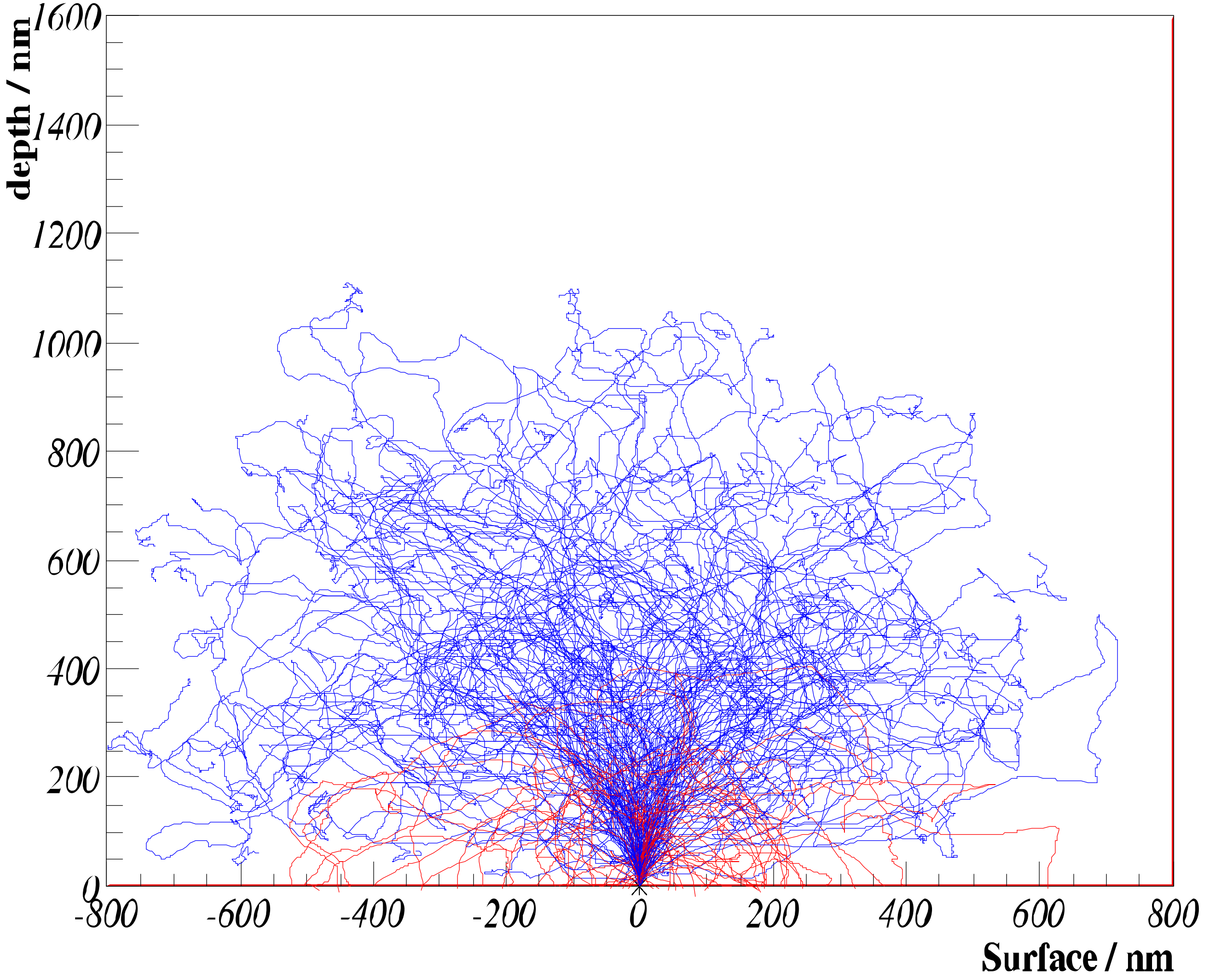

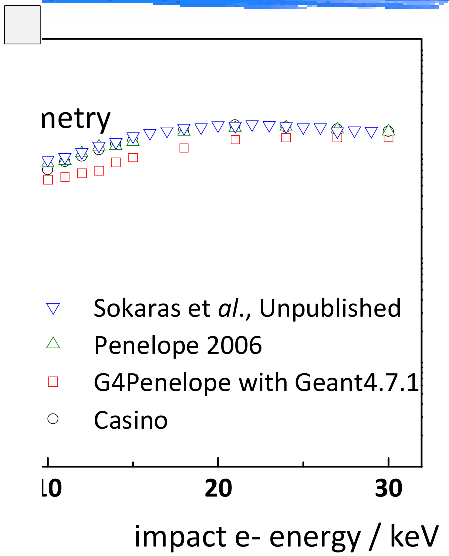

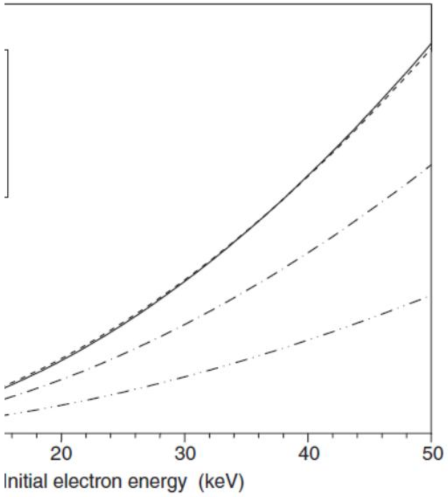

j_K ... $0.0115Z_K$ (keV) the mean ionization potential

Ionization induced by electrons

Stochastic movement of electrons (20 keV on Fe)

$$n_i(E_o) = \frac{N_A \rho W_i}{A_i} \int_{E_0}^{E_{Edge,i}} Q_i(E) \frac{1}{dE/_{ds}} dE$$

Green and Cosslett expression for the number of photons emitted by interaction with a single electron of initial kinetic energy Eo

$$Q_{ip}(E) = 6.51 \times 10^{-20} \frac{Z_{subshell,i}}{E_{Edge,i}{}^2} b \frac{ln(cU)}{U} \quad (cm^2)$$

$Q_i(E)$ and dE/ds are the inner shell ionization cross-section and the stopping power (energy loss function), respectively, of electrons in a material

$$\frac{dE}{ds} = -\frac{\rho}{J'} \sum_k \frac{W_k Z_k}{A_k} \frac{1}{1.18 \times 10^{-5} \sqrt{E/_{J'}} + 1.47 \times 10^{-6} \left(E/_{J'}\right)}$$

Love et al. expression for stopping power of electrons

$J_k = 0.0115 Z_k \ (keV)$ the mean ionization potential

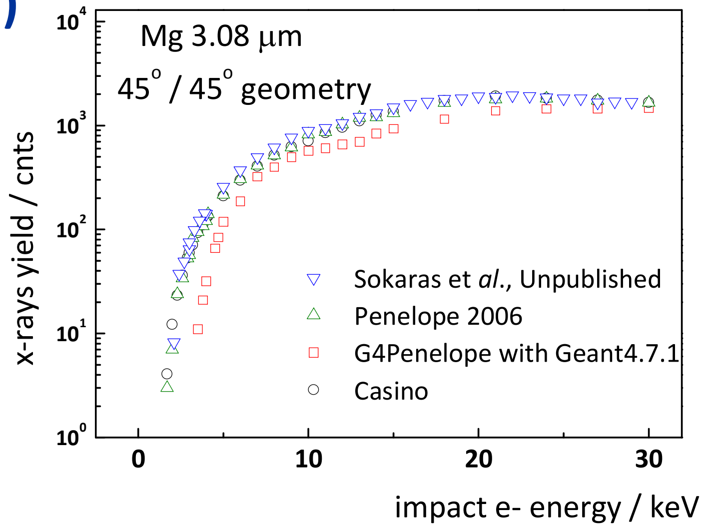

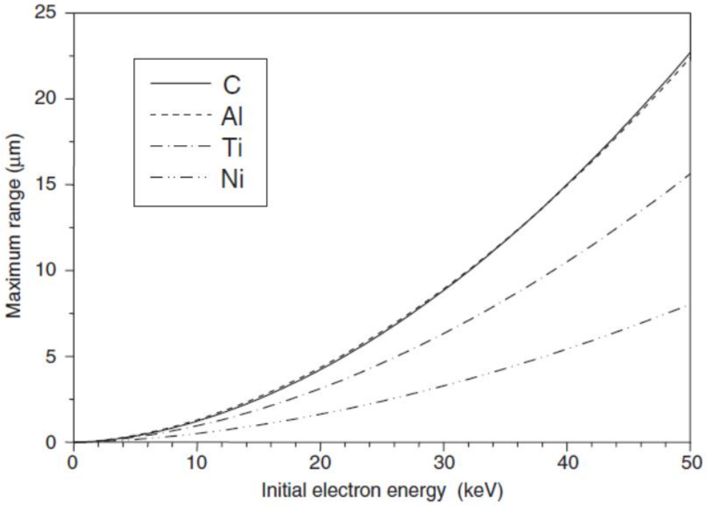

Photo e$^-$ Fluorescence Enhancement

$$N_{i,photo-electron} = G_i C_i \sum_j \int_{E=E_{Edge,j}}^{E=E_{max}} \frac{N_0(E)\tau_j n_i(E - E_{Edge,j})dE}{\mu^*}$$

Increases when exciting beam energy is far away from absorption edge of light elements

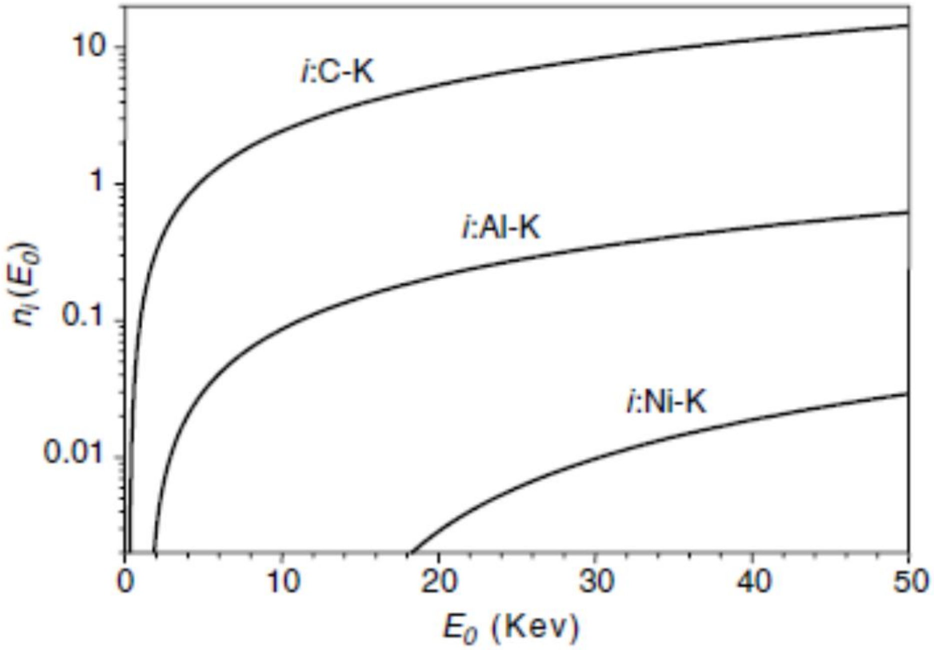

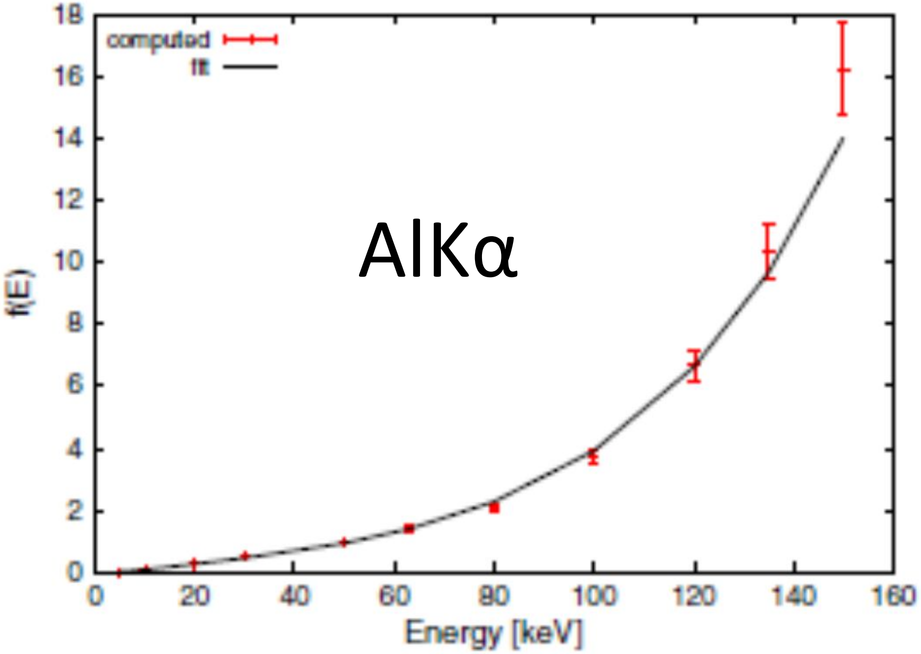

N. Kawahara in Handbook of Practical X-Ray Fluorescence Analysis, by B. Beckhoff B. Kanngiesser, N. Langhoff, R.Wedell, H.Wolff, (Eds.)

J. Fernandez et *al.*, X-Ray Spectrometry 2013, 42, 189–196

Photo e$^-$ Fluorescence Enhancement

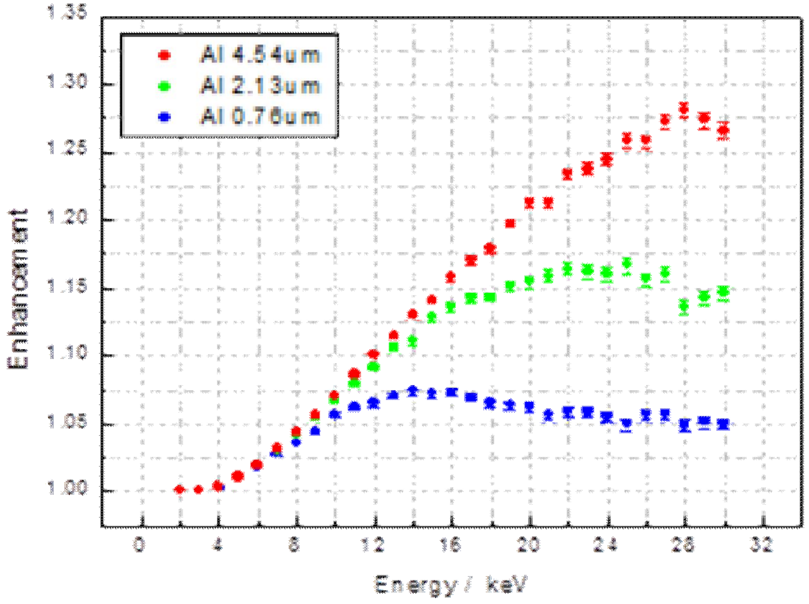

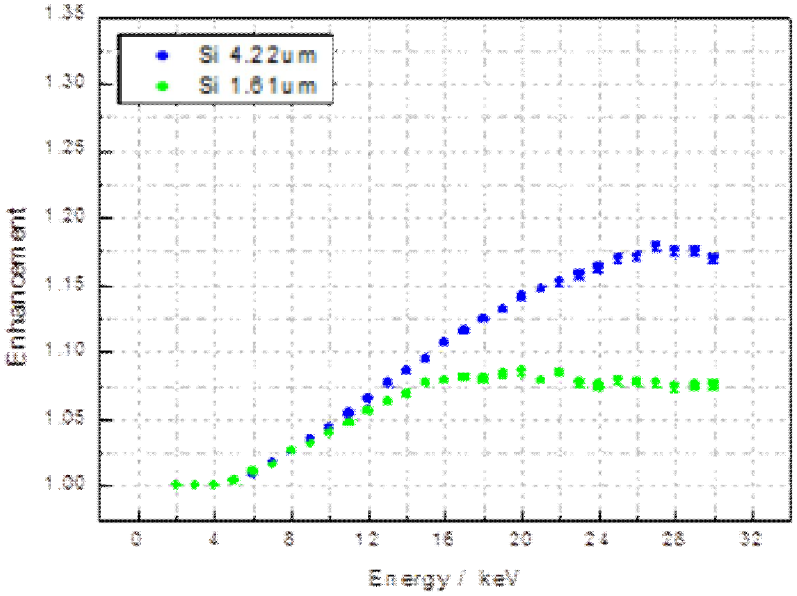

Monte Carlo calculations of phot-e enhancement:
Al (4.54µm, 2.13µm, 0.76µm) and Si (4.22µm, 1.61µm)
Casnati parameterization for electron ionization cross sections

D. Sokaras et *al.*, unpublished

Auger e$^-$ Fluorescence Enhancement

$$N_{i,Auger-electron} = G_i C_i \sum_j \int_{E=E_{Edge,j}}^{E=E_{max}} \frac{N_0(E)\tau_j(1-\omega_i)\sum_\kappa n_i\left(E_{Auger-electron,jk}\right)}{\mu^*} dE$$

- **Important:** When a light element analyte is embedded in a heavy element matrix.

- The Auger-electrons from the matrix elements can excite light element fluorescence.

- Example: When carbon in steel is analyzed, a Fe KLL Auger-electron with a kinetic energy of 6.3 keV can excite multiple carbon K-shells

Secondary electron induced ionizations

Example: Thick Fe target

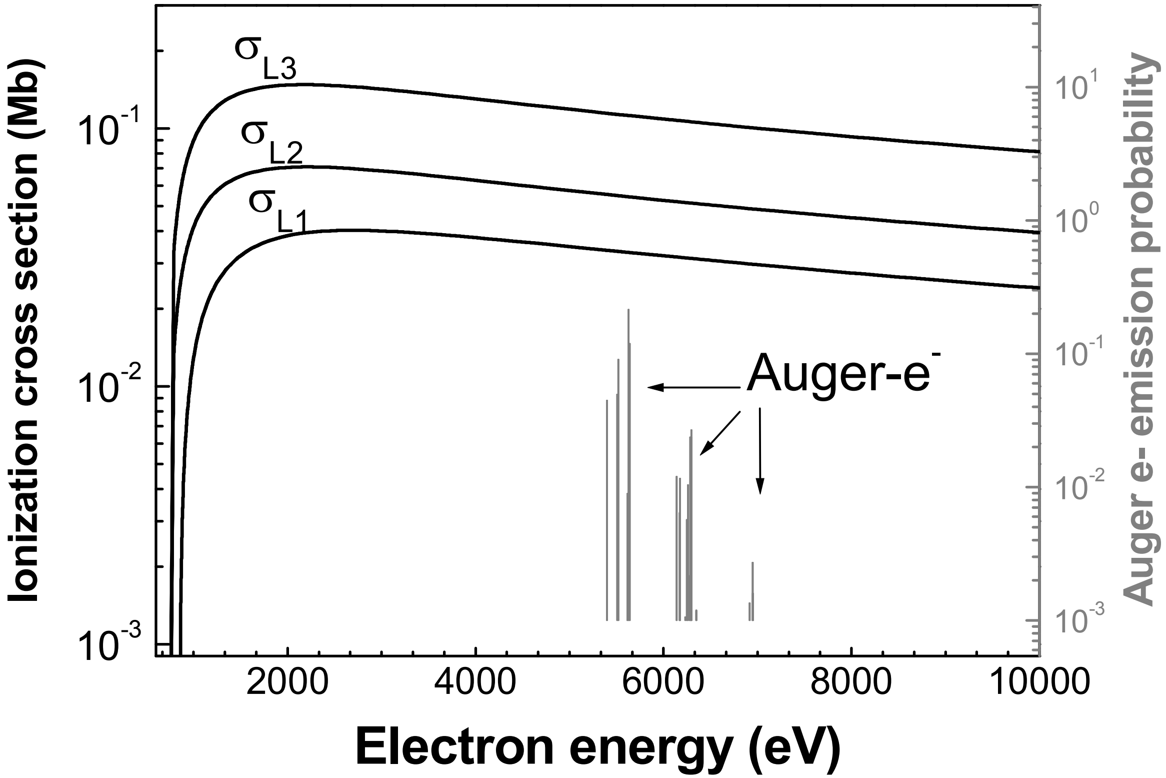

- **L-shell photoelectrons**: $T_e = E_o - U_{Li}$,
- **Auger-electrons** (when $E_o > U_K$)

Relative e- enhancement to Fe-Lα excitation in the case of a Fe pure target

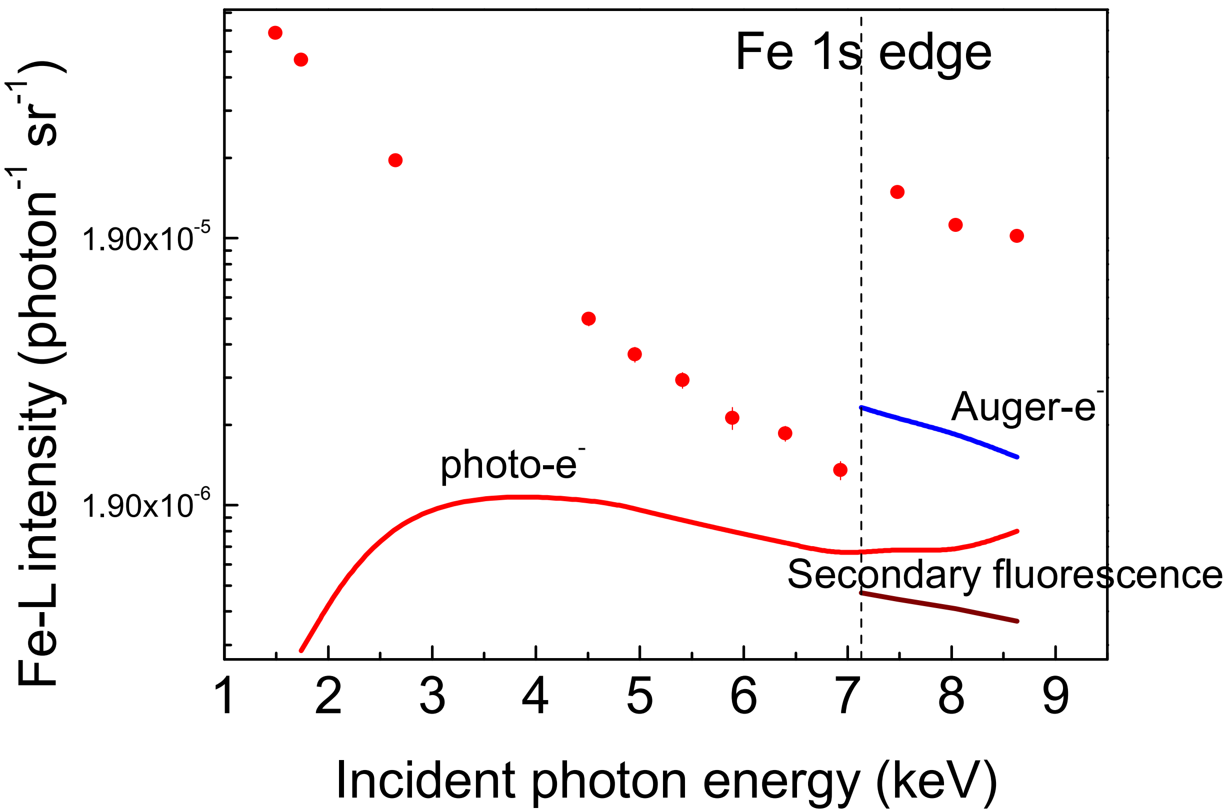

Bulk metallic Fe, Unpolarized incident radiation

Sokaras et *al*., Phys. Review A 83, 052511 (2011)

Compton electrons Fluorescence Enhancement

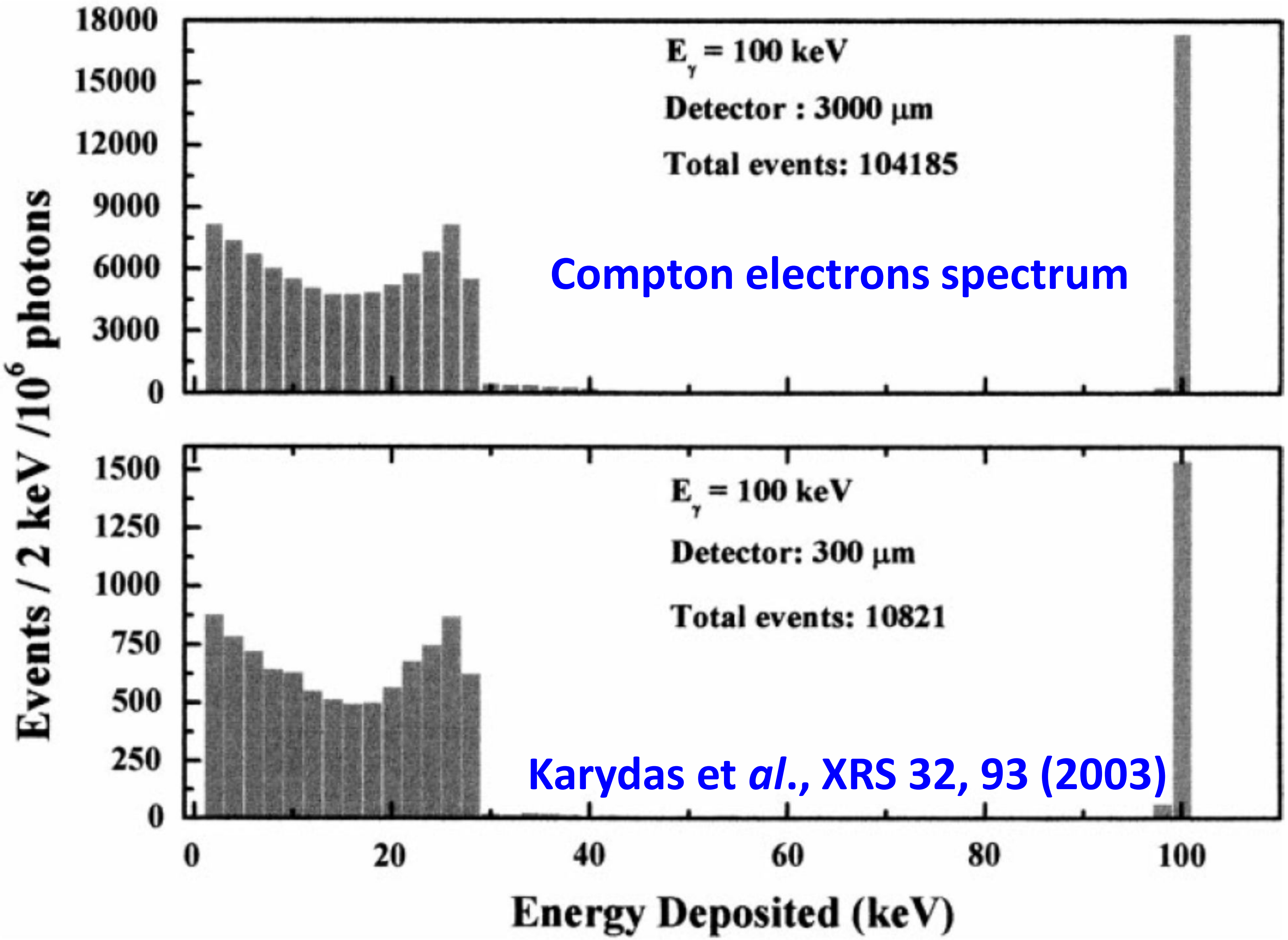

Compton electrons spectrum

Karydas et *al*., XRS 32, 93 (2003)

Compton electrons Fluorescence Enhancement

Thomas-Fermi model for the incoherent scattering function

$$\frac{\partial_a \sigma_{incoh}}{\partial \Omega} = \frac{\partial_c \sigma_{KN}(E_0, E', \theta)}{\partial \Omega} Z S(\alpha, \theta, Z)$$

$$S(v) = 1 - exp(-4.88 v^{0,856})$$

$$v = \frac{2}{3} \frac{137}{Z^{2/3}} asin(\theta/2)$$

$$\alpha = \frac{E_0}{m_c c^2}$$

Energy distribution of Compton electrons

$$\frac{\partial_a \sigma_{incoh}}{\partial E} = 2\pi Z r_0^2 \frac{m_c c^2}{E_0^2} \left[\frac{E_0^2 E_0 E + E^2}{E_0(E_0 - E)} + \left(1 - \frac{m_c c^2 E}{E_0(E_0 - E)} \right) \right] \left\{ 1 - exp \left[-1.11766 \times \left(\frac{E_0}{Z^{2/3}} \right) \sqrt{\frac{m_c c^2 E}{2E_0(E_0 - E)}} \right] \right\}$$

K. Stoev, J. Phys. D: Appl. Phys. 25 (1992) 131-138

Exciting beam : 59.6 keV, Sample: Fe_20_3 + ZnS

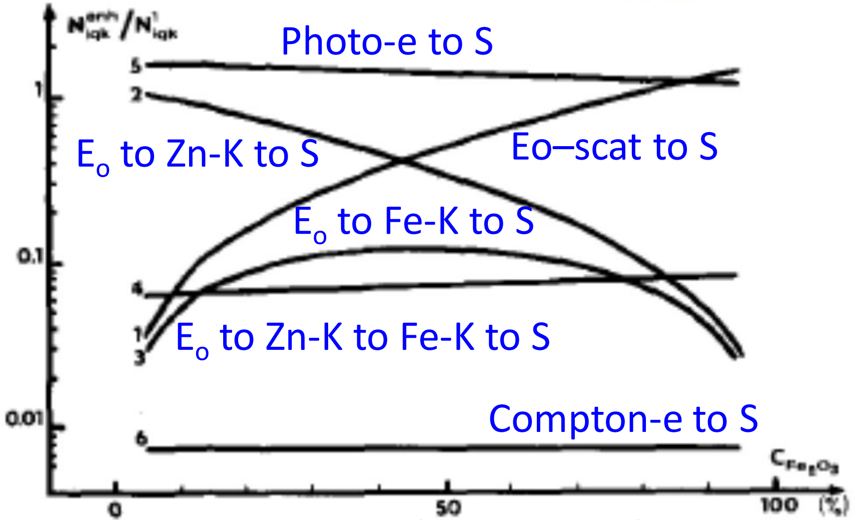

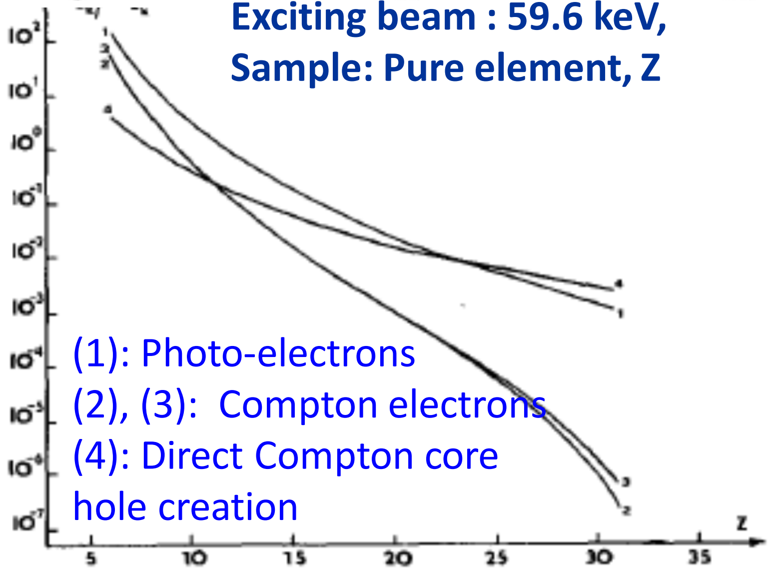
Exciting beam : 59.6 keV, Sample: Pure element, Z

De-excitation processes for inner-shell ionized atoms. Diagram L-emission

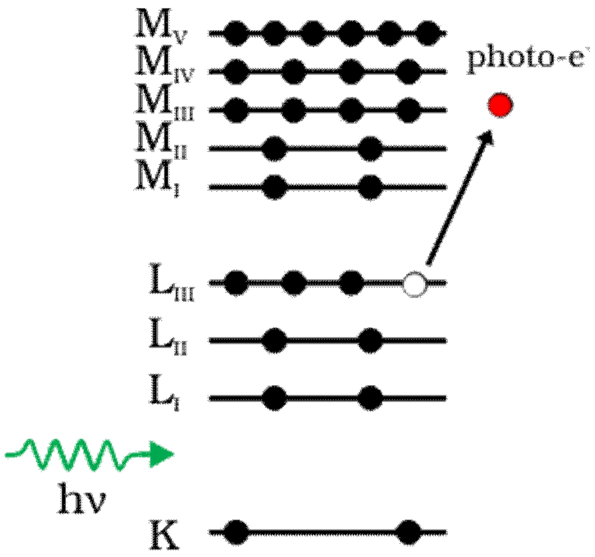

Photo-ionization

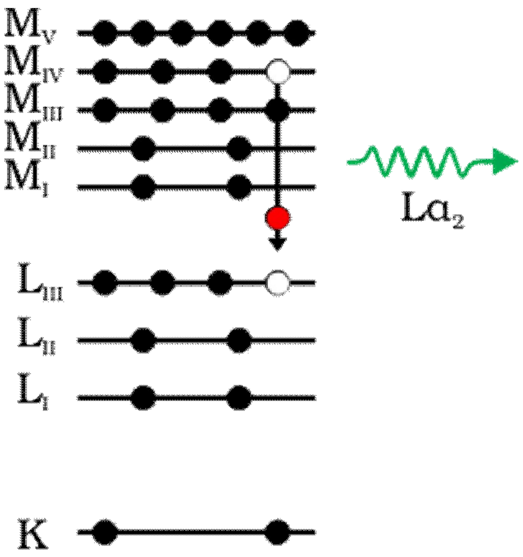

Fluorescence

Emission of a diagram line

Cascade L X-ray emission

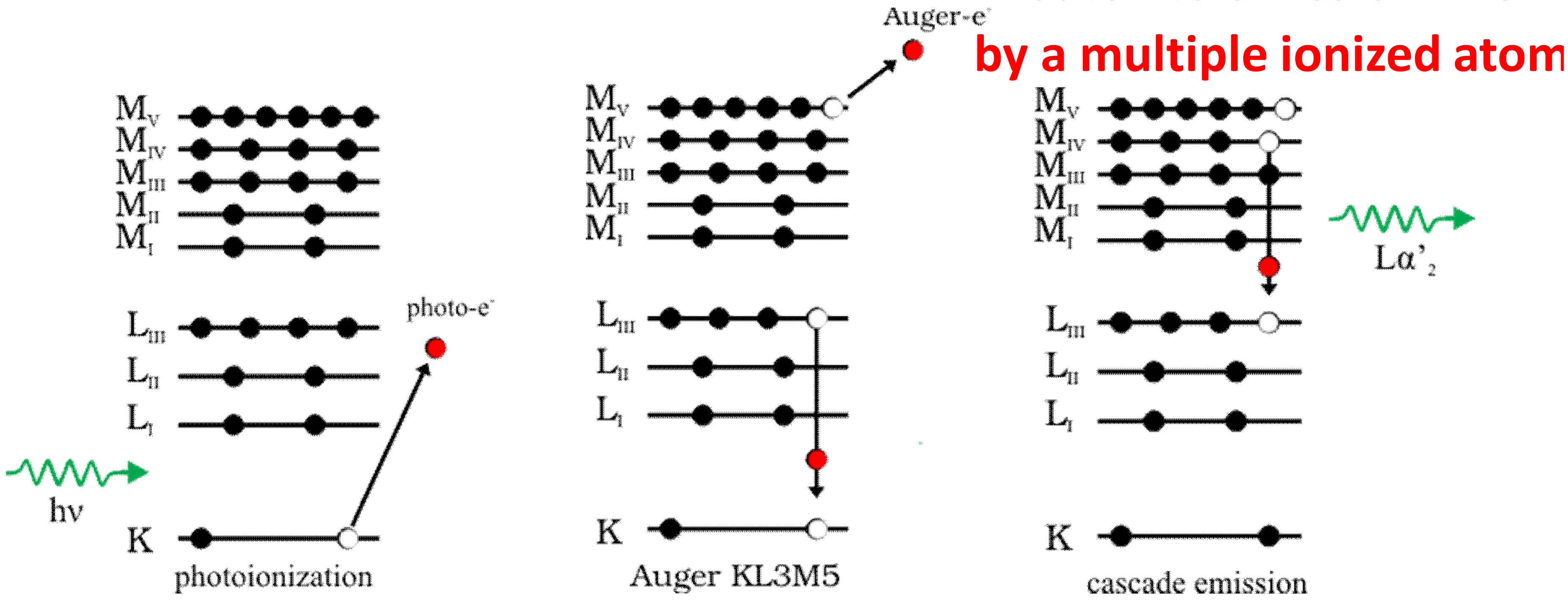

Cascade Emission: X-ray emission due to relaxation of an **indirectly** vacancy created by the relaxation of innermost shell and **not** due to a direct ionization.

Fe-L cascade effect

Bulk metallic Fe, Unpolarized incident radiation

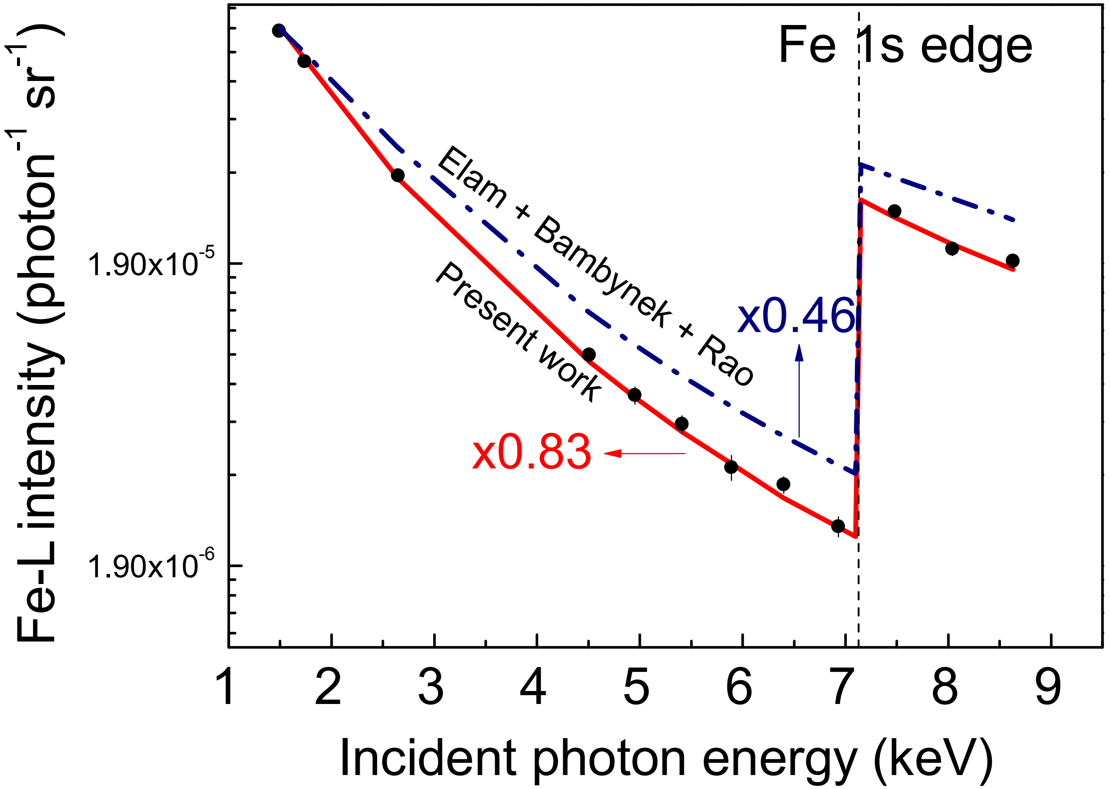

Sokaras et *al*., Phys. Review A 83, 052511 (2011)

T. Schoonjans et *al*, SAB, B66, (2011) 776

Fluorescence cross sections include full cascade effect due to radiative and non radiative probabilities

Secondary fluorescence enhancement

Z	WF (%)	Ipr (%)	Isec (%)	Iter (%)	Iscat (%)
Al	8.4	1	21.2	1.17	1.2
Si	26.7	1	18.1	0.64	1.23
Ca	9.3	1	13.8	-	1.64
Fe	9.8	1	-	-	2.44

$\psi_1 = \psi_2 = 45^o$

$E_0 = 17.44 keV$
$(Mo - K_a)$

Geometrical considerations: Non-parallel x-ray beams

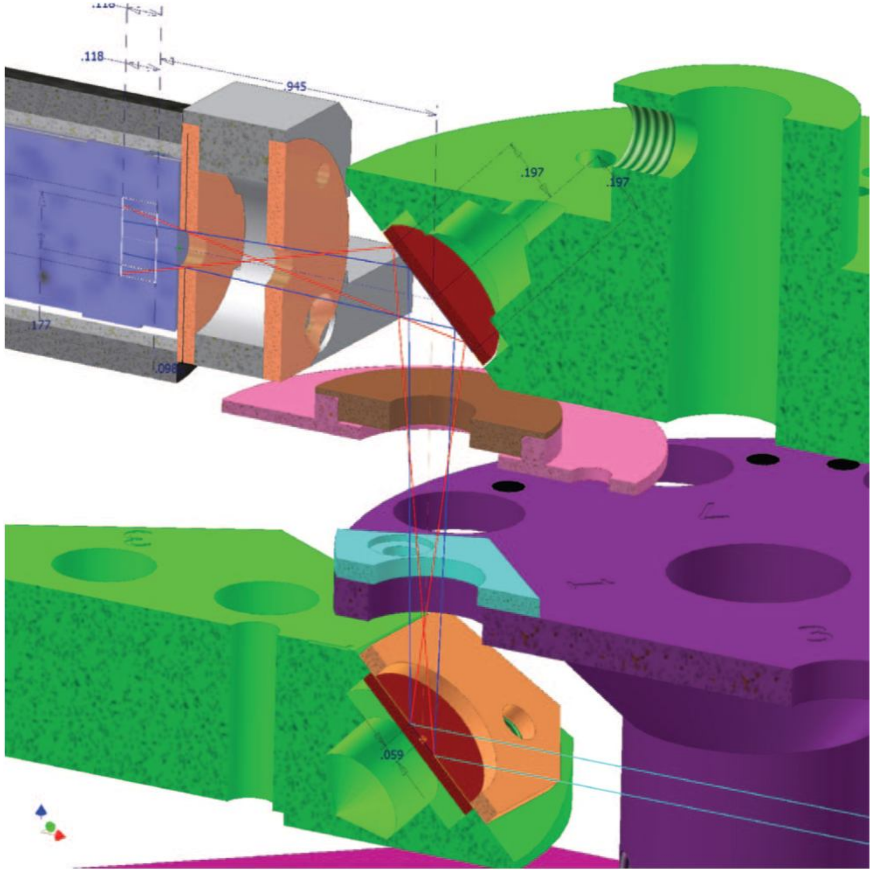

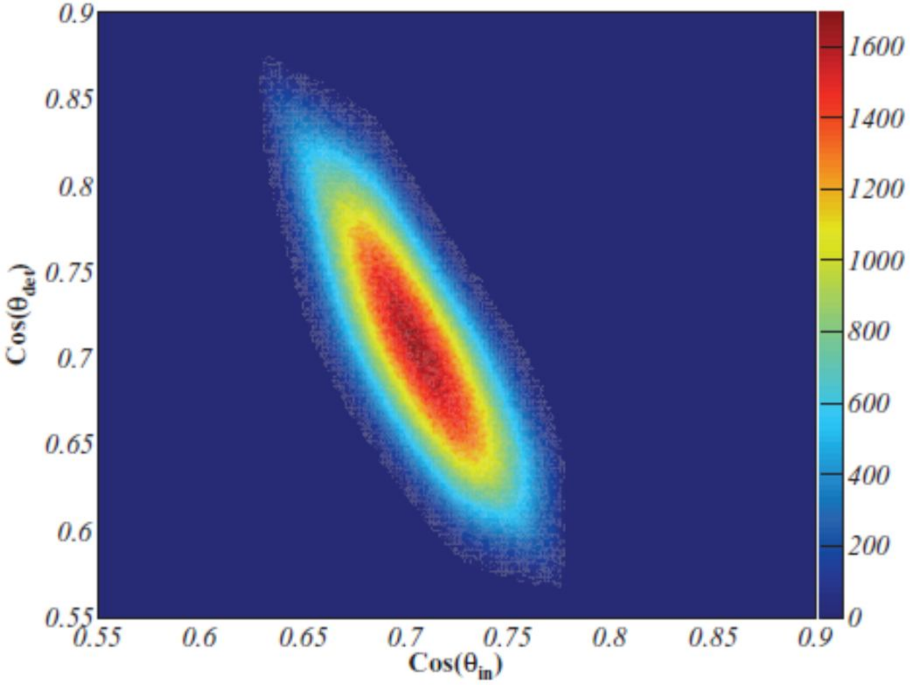

$\vartheta_{in}=45.2^\circ$ and $\vartheta_{out}=44.7^\circ$

Sokaras et al., Review of Scientific Instruments 83, 123102 (2012);

Fluorescence intensities for non-parallel x-ray beams

The divergent angle ¸ is 20° and the trajectories are distributed isotropically

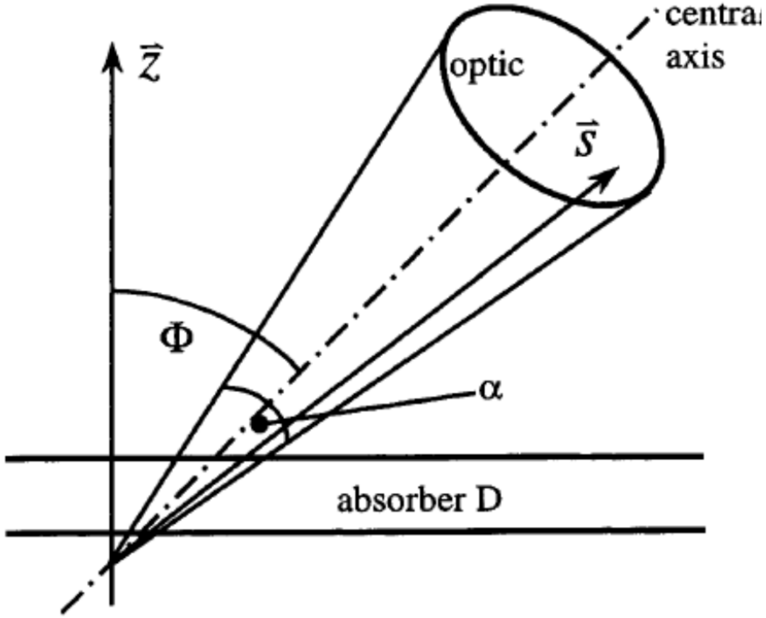

$$\left(\frac{I}{I_0}\right)^d = \int p(\vec{s})exp\left(\frac{-\mu\rho D}{s_z}\right)d\vec{s}$$

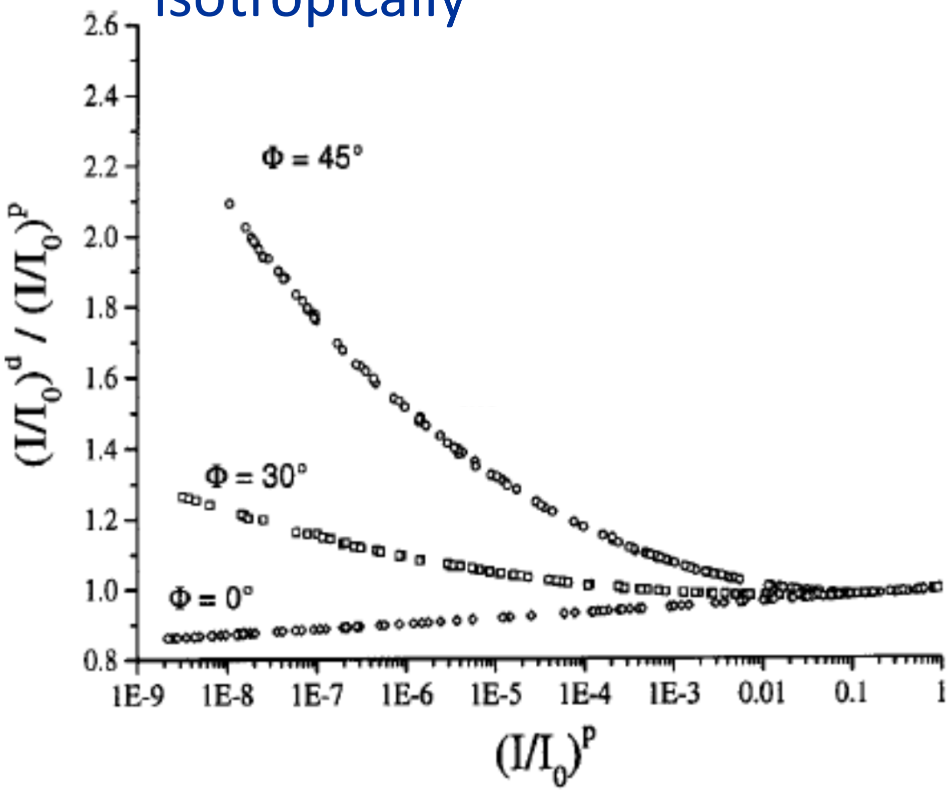

Malzer, Kanngiesser, X-Ray Spectrom. 2003; 32: 106–112

Fluorescence intensities for non-parallel x-ray beams

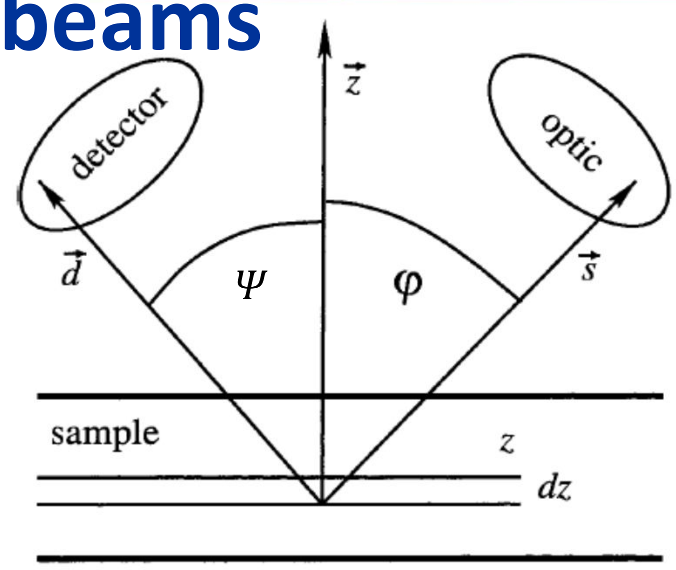

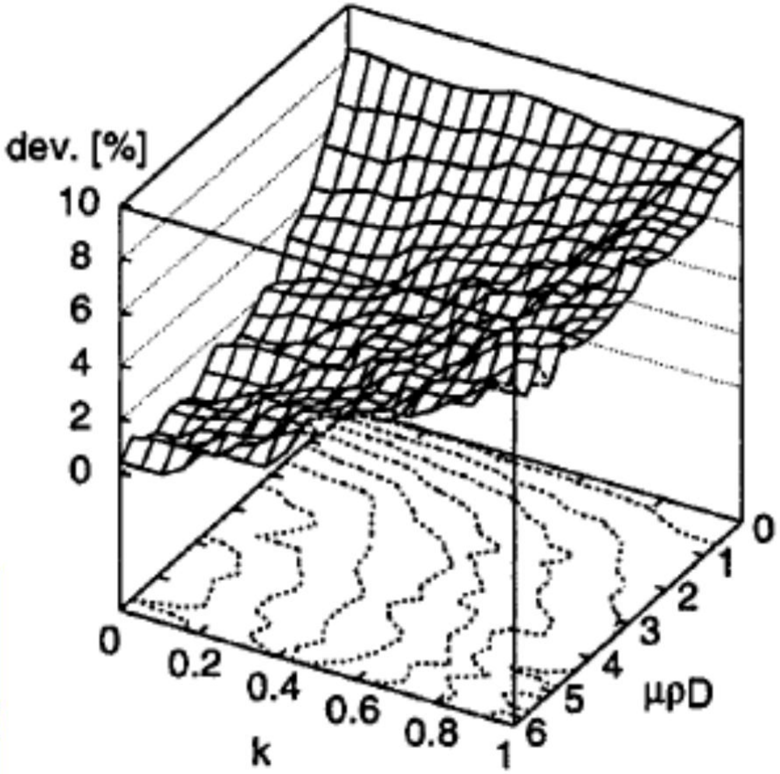

$$I_i^d = \frac{I_0 K_i c_i}{\mu} \int p(\vec{s})\, p(\vec{d}) \frac{1 - exp\left[-\mu\rho D\left(\frac{k}{d_z} + \frac{1-k}{s_x}\right)\right]}{k\frac{s_z}{d_z} + (1-k)} d\vec{s} d\vec{d}$$

$$\cos = s_z \;\; and \;\; \cos\Psi = d_z$$

$$\mu = \mu_0 + \mu_i$$

$$k = {}^{\mu_i}/_{\mu}$$

The divergent angle of the excitation is 60°, inclined to 20°. The detector again covers 20°, inclined to 30°. XRF and micro-XRF spectrometers which employ Bragg optics

A polycapillary lens, with a divergent angle of 10°, pointing perpendicular towards the sample surface. Detector angle of 20°.

Geometrical considerations in XRF intensities

Incident flux I_o is expressed in number of photons/s/cm^2

$$G = \frac{\Delta\Omega}{4\pi} \times \frac{w d_s}{a^2} \sin\vartheta_1$$

$$G = \frac{\Delta\Omega}{4\pi} \times \frac{w d_2}{a^2} \times \frac{\sin\vartheta_1}{\sin\vartheta_2}$$

$$G = \frac{\Delta\Omega}{4\pi} \times \frac{w d_o}{a^2}$$

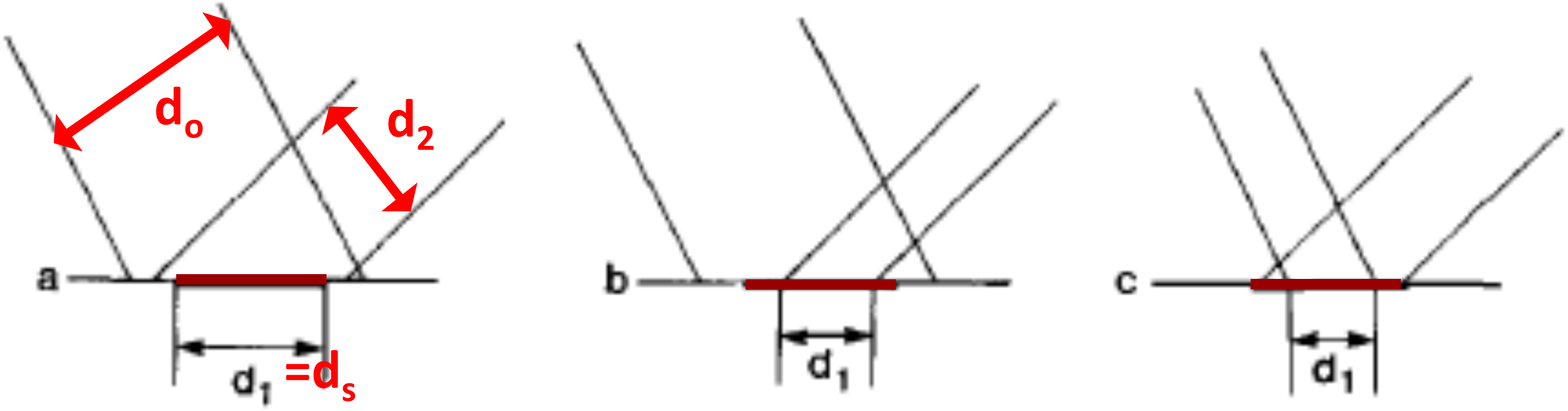

$$G \propto \sin\vartheta_1$$

$$G \propto \frac{\sin\vartheta_1}{\sin\vartheta_2}$$

$$G = const$$

De Boer, XRS, 18, 119, 1989

Geometrical considerations in XRF intensities

Geometry under **GI conditions**

$$\Omega = \int_{-\infty}^{\infty} I(x)\,d\Omega(x)\,dx$$

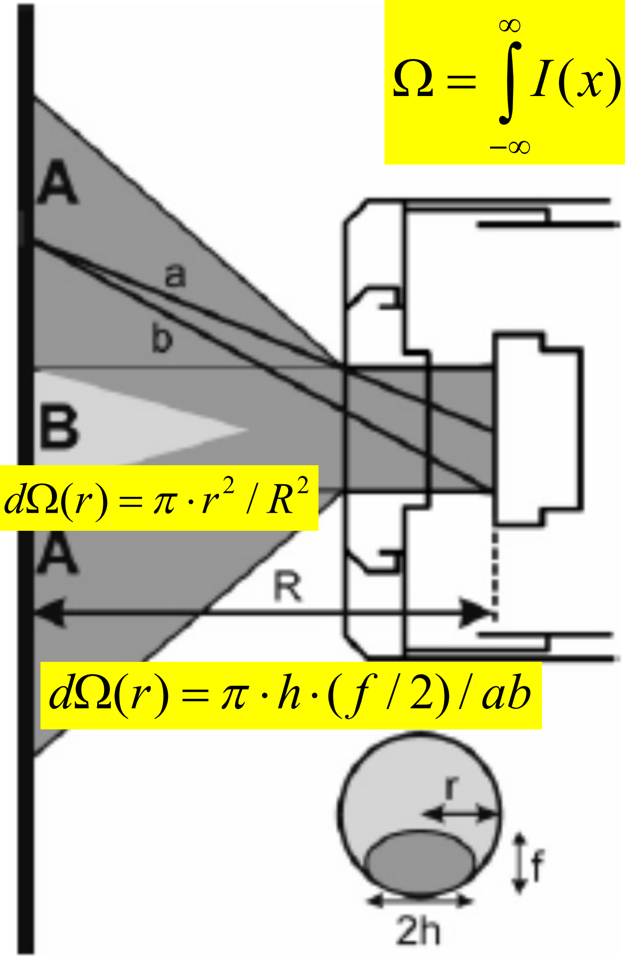

$$d\Omega(r) = \pi \cdot r^2 / R^2$$

$$d\Omega(r) = \pi \cdot h \cdot (f/2)/ab$$

B. Beckhoff et al Anal. Chem. 2007

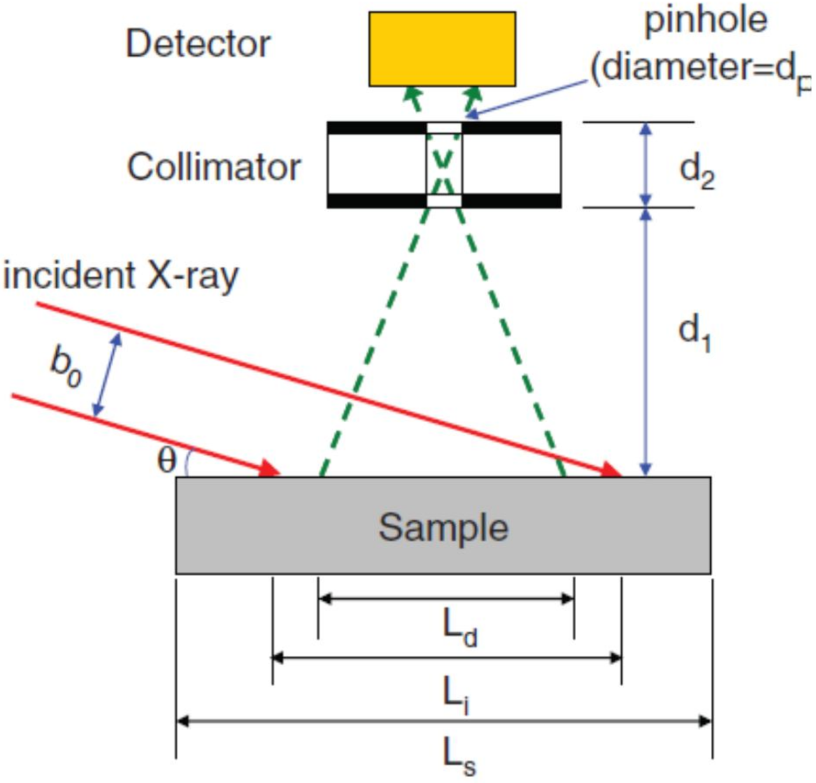

Weblin Ll, Rev. Sci. Instrum. 83, 053114 (2012); doi: 10.1063/1.4722495

Geometrical considerations in XRF intensities

Sample Volume effect in milli-beam size XRF set-ups

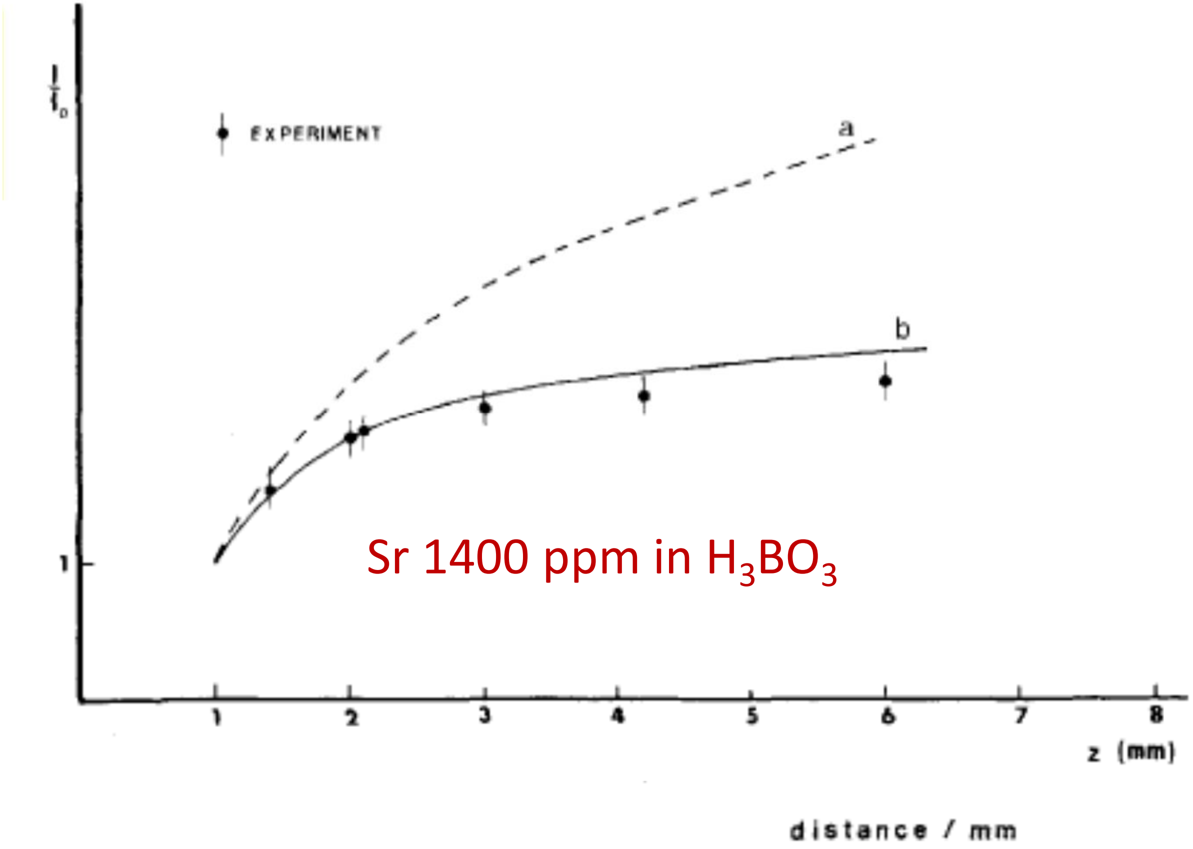

Sr 1400 ppm in H_3BO_3

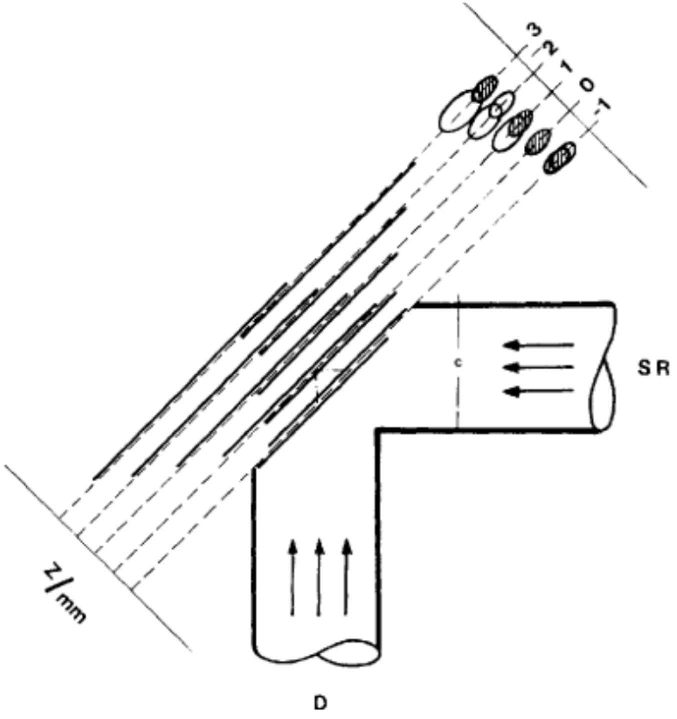

Orlic et al. XRS, 16, 125-130 (1987)

Effect of Surface Topography in XRF intensities

$$N_i = \frac{K_i C_i}{\sin(\varphi_1 + \theta)} \left(\sum_E \frac{\tau_{i,E}}{\mu'_{S,E} + \mu^N_{S,i}} I(E)\Delta E + \sum_j \sum_J C_j \, g_J \tau_{i,j} \times \sum_E \frac{\tau_{j,E} I(E)\Delta E}{\mu'_{S,E} + \mu^N_{S,i}} L_{i,J} \right)$$

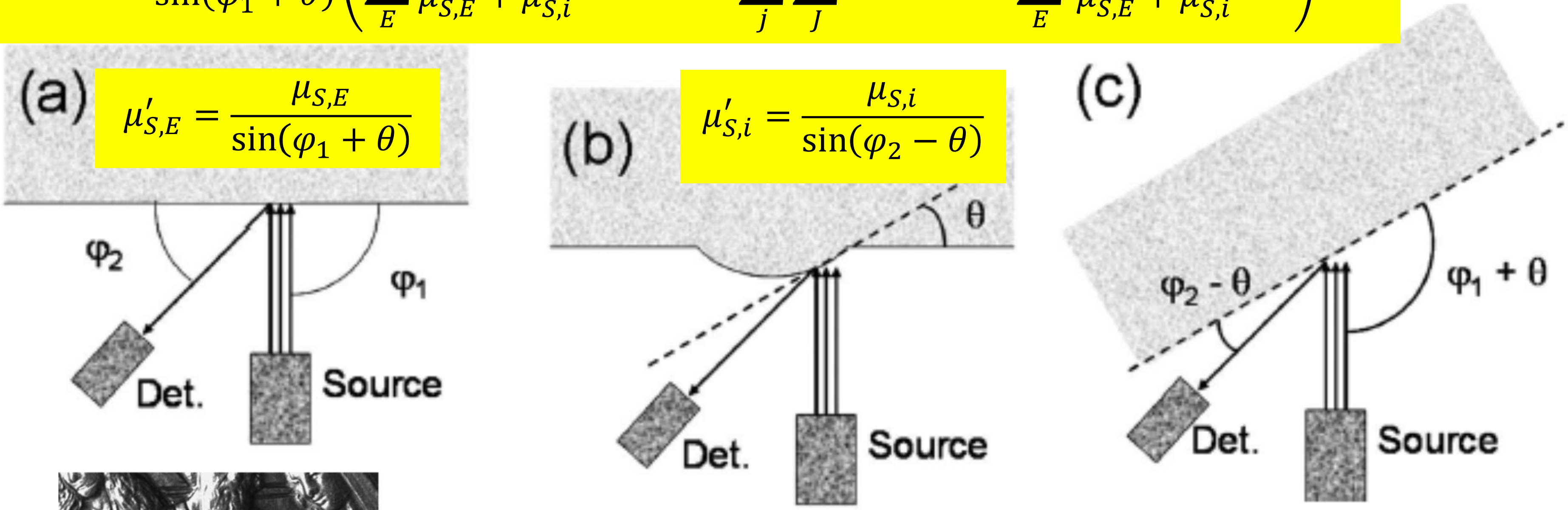

$$\mu'_{S,E} = \frac{\mu_{S,E}}{\sin(\varphi_1 + \theta)}$$

$$\mu'_{S,i} = \frac{\mu_{S,i}}{\sin(\varphi_2 - \theta)}$$

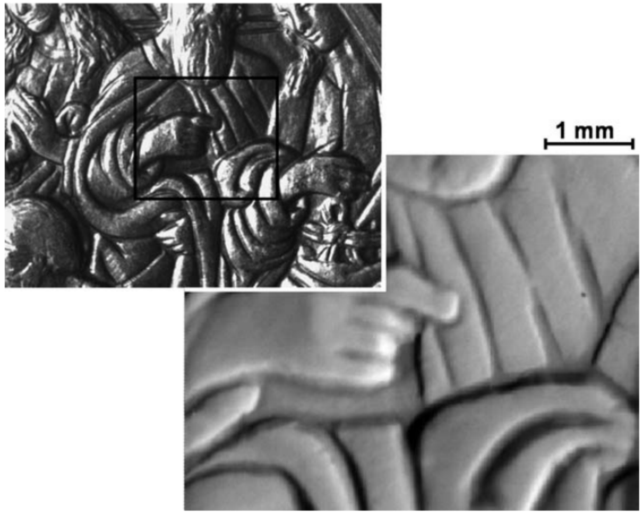

T. Trojek, J. Anal. At. Spectrom., 2011, 26, 1253

Effect of Surface Topography in XRF intensities

$$\hat{n}\cdot\left(s_i\hat{b}+s_f\hat{d}\right)=0$$

$$s_f=-\frac{\hat{b}\cdot\hat{n}}{\hat{d}\cdot\hat{n}}s_i\equiv k\cdot s_i$$

$$k=(\cos a+\tan\theta\sin\alpha)^{-1}$$

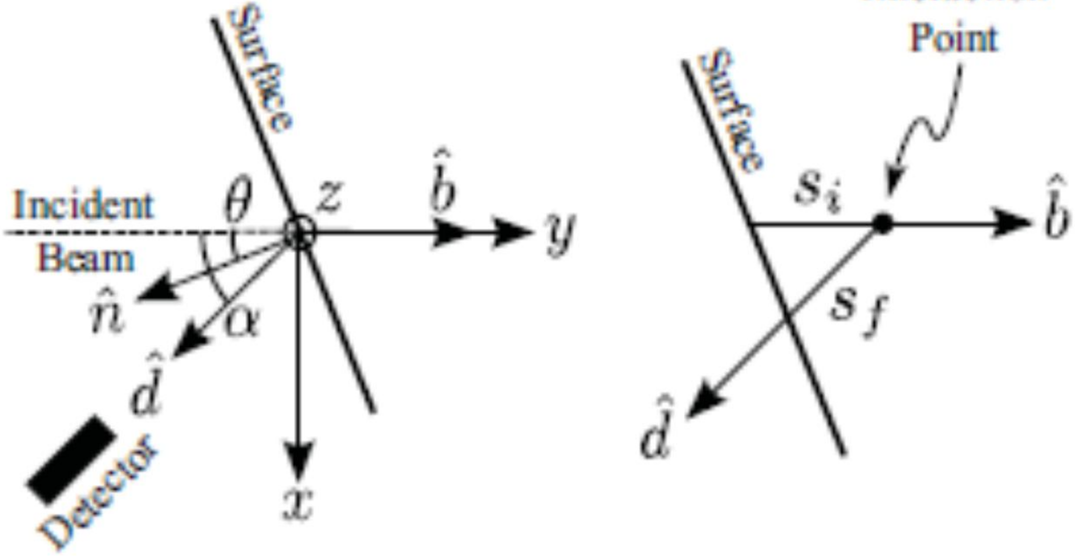

$$I=\lambda\int_0^{\infty}exp\left[-\left(\mu_i+k\mu_f\right)s_i\right]ds_i=\frac{\lambda}{\mu_i+k\mu_f}$$

$$I(\theta)\propto\frac{1}{1+\left({}^{\mu_f}/_{\mu_i}\right)(\cos a+\tan\theta\sin a)^{-1}}$$

ϑ is the rotation of the surface normal around the *z* axis; $\vartheta = 0$ for a surface parallel to the *xz* plane

E. C. Geil and R. E. Thorne, J. Synchrotron Rad. (2014), 21, 1358-1363

Effect of Surface Topography in XRF intensities

Hints:
The objects should be mounted so that their dominant surface curvature runs perpendicular to the detector–incident beam (x-y) plane

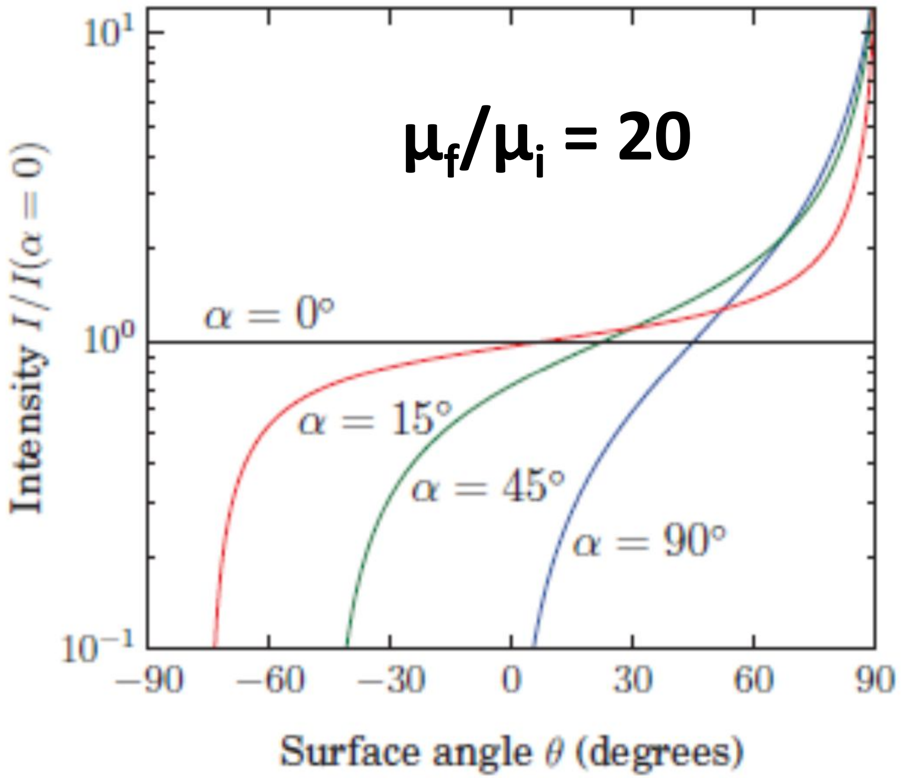

The angle effect vanishes as the detector position approaches the incident beam, and it is maximal when the detector is perpendicular to the beam. $CaCO_3$ matrix, with incident beam energy 16.5keV

Effect of Surface Topography in XRF intensities

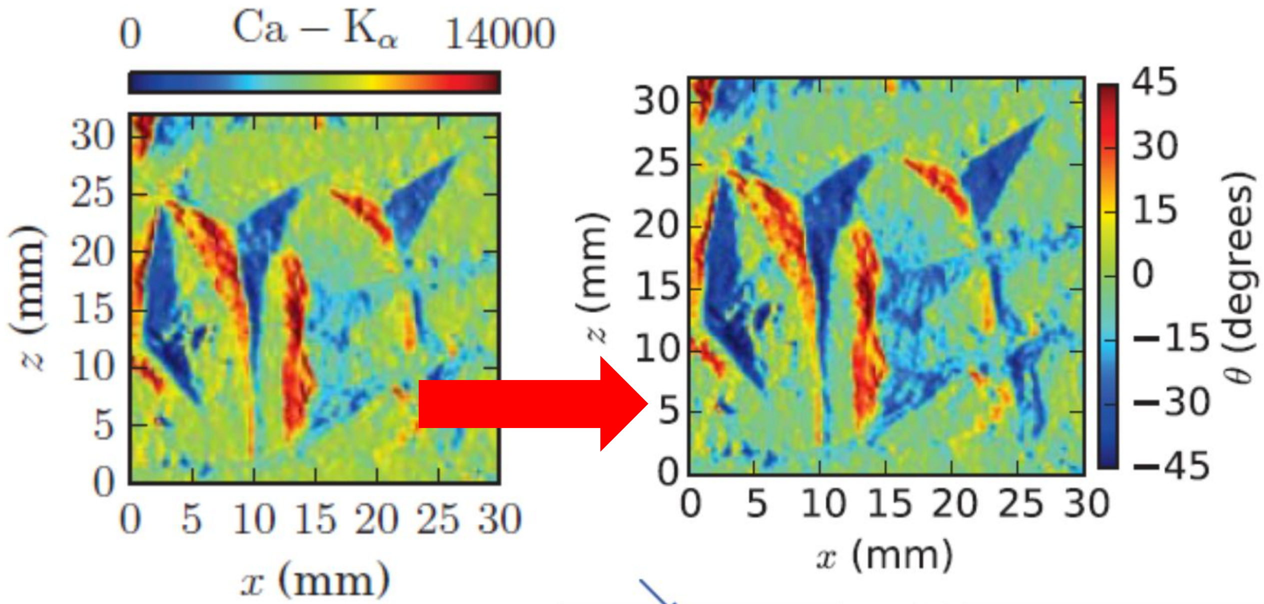

Map of surface angle θ computed from the Ca – Kα fluorescence

Rendering of the scanned area and shaded as if obliquely illuminated from the right side by a light source.

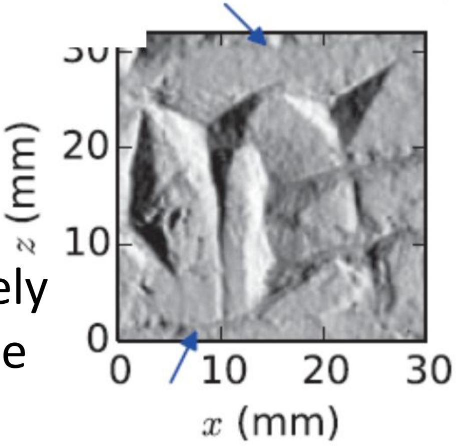

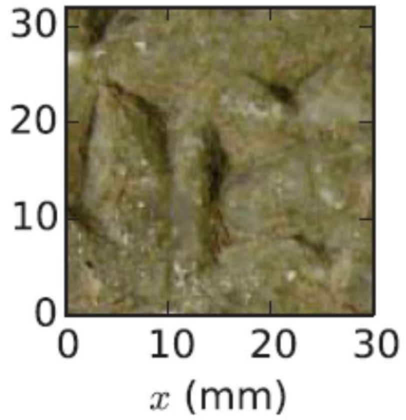

Photograph of the scanned area, adjusted to enhance contrast and brightness.

Sample effects – Particle size

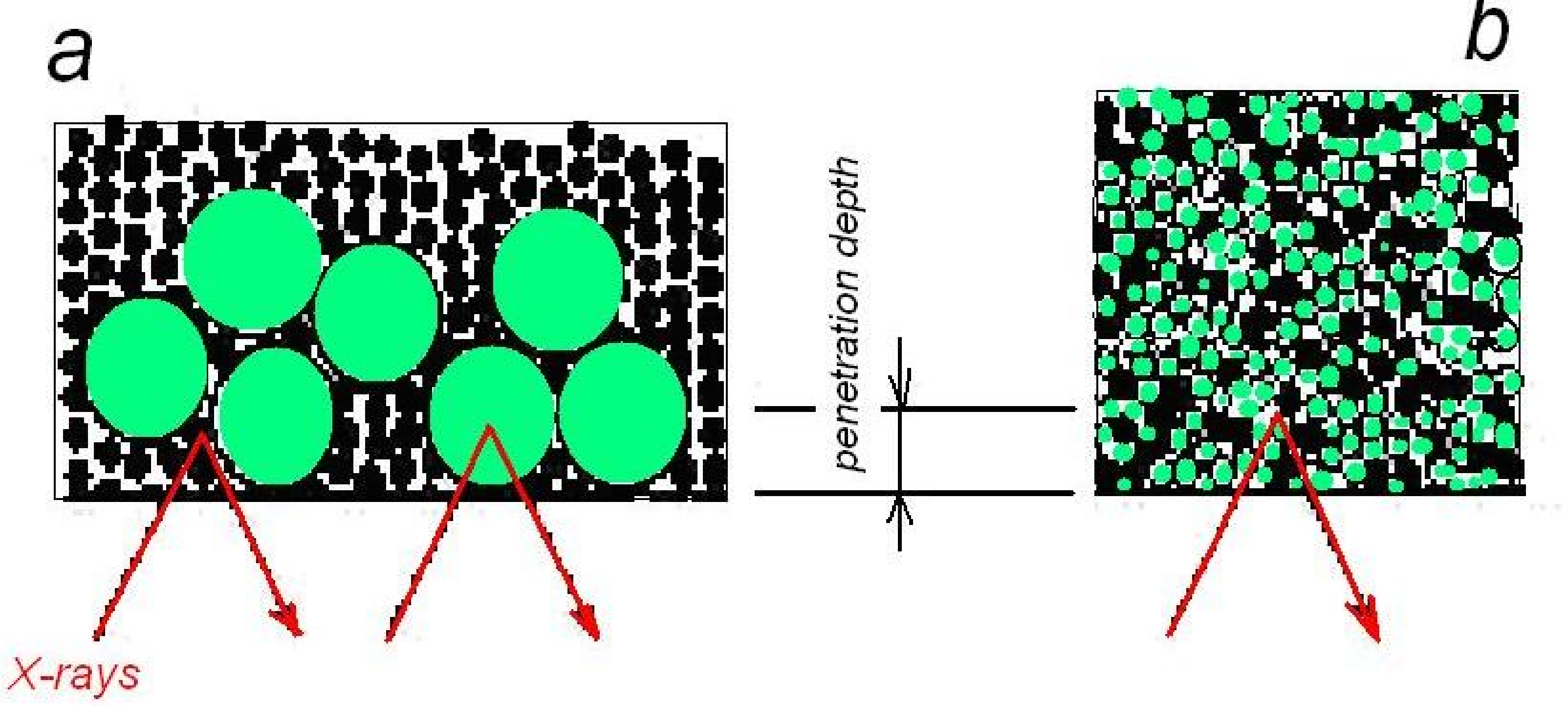

Example: Fe2O3

50% of 8 -12 keV from 30µm – 60µm

90% of 8 -12 keV from 100µm – 200µm

Information originates only from the first two layers

Particle size correction models

- Berry et al (Adv. X-ray Anal. 12, 612 1969)
  - Dependence of fluorescence intensity on:
    - $\bar{d}$ =2/3 diameter of sphere
    - η =packing ratio, $m = \frac{c_{nf}}{c_f}$ $\quad D \approx 10nm$

$$P_{ja} = \frac{1 - \exp\left[(\mu_f + \mu_f^{'}) \cdot \rho_f \cdot \bar{d}\right]}{1 - \exp\left[(\mu_f + \mu_f^{'}) \cdot \rho_f \cdot D\right]} \cdot \frac{\left\{1 - \eta + \eta \cdot \exp(-\mu_f \cdot \rho_f \cdot D) + \eta \cdot m \cdot \exp(-\mu_{nf} \cdot \rho_{nf} \cdot D)\right\}}{\left\{1 - \eta + \eta \cdot \exp(-\mu_f \cdot \rho_f \cdot \bar{d}) + \eta \cdot m \cdot \exp(-\mu_{nf} \cdot \rho_{nf} \cdot \bar{d})\right\}}$$

$$\mu_f = \sum_f c_f \frac{\mu_f(E_0)}{\sin\psi_1} \qquad \mu_{nf} = \sum_{nf} c_{nf} \frac{\mu_{nf}(E_0)}{\sin\psi_1}$$

$$\mu_f^{'} = \sum_f c_f \frac{\mu_f(E_j)}{\sin\psi_2} \qquad \mu_{nf}^{'} = \sum_{nf} c_{nf} \frac{\mu_{nf}(E_j)}{\sin\psi_2}$$

Overview - Conclusions

- The quantitative XRF analysis is currently supported by a well-defined mathematical formalism based on the so-called fundamental parameters approach
- The majority of second/third order phenomena that affect the analyte fluorescence intensity are described by analytical formulas

Obstacles:

- ✓ Enhancement due to electrons ionization requires verification and currently is not taken into account routinely
- ✓ Accuracy of fundamental parameters (soft energy region) and for L, M characteristic X-rays

Perspectives

- ☐ Monte Caro methods it is the most comprehensive tool to account for all high-order phenomena and assess their contribution in fluorescence intensities
- ☐ FP re-evaluation by means of metrological SR experiments

Acknowledgements

- ✓ Charalambos Zarkadas, PANalytical B.V. , The Netherlands
- ✓ Dimosthenis Sokaras, Stanford Synchrotron Radiation Lightsource, USA
- ✓ Vasiliki Kantarelou, INPP, NCSR “Demokritos”, Greece